



HAL
open science

Optimal Control of the Controlled Lotka-Volterra Equations with Applications - The Permanent Case

Bernard Bonnard, Jérémy Rouot

► **To cite this version:**

Bernard Bonnard, Jérémy Rouot. Optimal Control of the Controlled Lotka-Volterra Equations with Applications - The Permanent Case. SIAM Journal on Applied Dynamical Systems, 2023, 22 (4), pp.2761-2791. 10.1137/22M151978X . hal-03757060v2

HAL Id: hal-03757060

<https://inria.hal.science/hal-03757060v2>

Submitted on 4 Jul 2023

HAL is a multi-disciplinary open access archive for the deposit and dissemination of scientific research documents, whether they are published or not. The documents may come from teaching and research institutions in France or abroad, or from public or private research centers.

L'archive ouverte pluridisciplinaire **HAL**, est destinée au dépôt et à la diffusion de documents scientifiques de niveau recherche, publiés ou non, émanant des établissements d'enseignement et de recherche français ou étrangers, des laboratoires publics ou privés.



Distributed under a Creative Commons Attribution 4.0 International License

Optimal Control of the Controlled Lotka-Volterra Equations with Applications. The Permanent Case*

Bernard Bonnard[†] and Jérémy Rouot[‡]

Abstract. In this article motivated by the control of complex microbiota in view to reduce the infection by a pathogenic agent, we introduce the theoretical frame from optimal control to analyze the problem. Two complementary approaches can be applied in the analysis: one is the so-called permanent case, where no digital constraints are concerning the control (taken as a measurable mapping) versus the sampled-data control case taking into account the logistic constraints, e.g. frequency of the medical interventions. The model is the n -dimensional Lotka-Volterra equation controlled using either probiotics or antibiotic agents or transplantation and bactericides. In this article, we concentrate to the permanent case associated to probiotic or antibiotic agent. The Maximum Principle is used to parameterize the geodesics and the optimal synthesis boils down to analyze mainly the singular trajectories and their concatenation with bang arcs.

Key words. Optimal control in the permanent case, biomathematics and population dynamics, geometric control theory.

MSC codes. 49K15, 92B05, 93C10, 93C15, 92D25

1. Introduction. The book by Vito Volterra [28] "Leçons sur la théorie mathématique pour la lutte pour la vie" leads to the Lotka-Volterra model to predict in a general frame the evolution on interacting biological species. The problem was studied independently by Lotka which makes the connection with chemical networks. The relation with control systems was already present in the original predator-prey model with two species set by Umberto D'Ancona to explain the evolution of the species in relation with reduction of the fishing activity during the first World War. The original memoir [28] starts with an interesting discussion about the evolution of the species in relation with integrability properties of the conservative model. It validates D'Ancona observations and opens the road to analyze different problems of populations dynamics. This leads to extend the model to the non conservative $2d$ -case in any dimension.

Recently our attention was attracted by the works of Jones et al. [17] based on the model by Stein et al. [27] in an attempt to model and cure a gut mouse microbiota infected by the *C. difficile* bacteria which leads to a 11-dimensional controlled Lotka-Volterra model, using either fecal transplantation or one antibiotic agent. The problem is analyzed using $2d$ -reduced (projection) non conservative Lotka-Volterra model. This model validates the effect of an antibiotic agent prior to infection and followed by a single fecal injection to cure the infection by constructing a separatrix which allows to decide about success or failure of the

*Submitted to the editors DATE.

Funding: This work benefited from the support of the FMJH Program PGMO and from the support of EDF; Thales, Orange and by the program PEPS "Jeunes chercheurs et jeunes chercheuses" of Insmi.

[†]Institut Mathématique de Bourgogne, Université de Dijon, 9 rue Alain Savary, 21078 Dijon and Inria Sophia Antipolis Equipe McTao (bernard.bonnard@u-bourgogne.fr).

[‡]Laboratoire de Mathématiques de Bretagne Atlantique, UMR 6205, 6 avenue Le Gorgeu, 29238 Brest (jeremy.rouot@univ-brest.fr).

36 procedure due to delay in the transplantation or insufficient dosing.

37 To understand this approach let us introduce the Lotka–Volterra dynamics and analyze
38 its limits, already discussed in [28]. The system is given by the equations

$$39 \quad (1.1) \quad \frac{dx}{dt}(t) = (\text{diag}(x(t)))(Ax(t) + r),$$

40 where $x = (x_1, x_2, \dots, x_n)^\top$ belongs to the positive quadrant $x_i \geq 0$ and is the vector of popu-
41 lations of the interacting species, $\text{diag}x$ denotes in short the diagonal matrix with coefficients
42 x_i , $A = (a_{ij})$ is the matrix containing the interacting coefficients between the species and
43 $r = (r_1, r_2, \dots, r_n)^\top$ is the vector describing the individual growth rate without interaction.
44 Assuming the matrix A invertible, the system possesses a unique interior equilibrium given by
45 $x_0 = -A^{-1}r$. The model is only valid provided that each species is contained in an interval
46 $[\varepsilon, M]$, $\varepsilon > 0$ and hence in the model only the so-called persistent trajectories defined for
47 positive times and contained in $[\varepsilon, M]^n$ have physical signification. Therefore the differential
48 equation represents an analytic continuation of the dynamics to the whole euclidean space.
49 But the model in fine describes the interaction between the interior equilibrium and equilibria
50 of an hierarchy of reduced Lotka–Volterra dynamics associated to extinction of the different
51 species, e.g. extinction of x_1 leads to analyze the reduced model of $n - 1$ interacting species
52 where we substitute in the dynamics $x \rightarrow x = (x_2, \dots, x_n)^\top$ and again we can compute the
53 interior equilibria of the reduced dynamics. Therefore this leads to interpret the model as a
54 system of interaction between a given number k of isolated equilibria with $k \leq 2^n$.

55 From this point of view the analysis of [17] is precisely to describe a policy in the ex-
56 perimental setting where a mouse is treated prior to infection by antibiotic and a final fecal
57 injection in order to cure the *C. difficile* infection. The $2d$ -reduced model is with a saddle
58 interior point with stability and unstability domain delimited by separatrixes and the success
59 of the therapy is to reach a stability domain of an healthy equilibrium.

60 At this time the connection with the network of chemical species pointed by Lotka has
61 to be made in relation with intense research activities in the seventies. They were motivated
62 by the analysis of chemical batch reactors and realized mainly by Feinberg–Horn–Jackson, see
63 for instance the recent book [15]. The study is related to the graph of the reactions using the
64 concept of deficiency.

65 Similarly concerning the Lotka–Volterra equations there was an intense research activities
66 due in particular to Zeeman, Smale, Hirsch to analyze the dynamics in the frame of the theory
67 of dynamical systems [29, 16, 26], the limit of the studies being related to complex chaotic
68 behaviors, see [3] for a seminal presentation of the computational complexity of the problem.

69 The analysis from geometric optimal control viewpoint of the problem of reducing the
70 infection of a complex microbiote using the Lotka–Volterra model leads to introduce the
71 polysystem $D = \{X, Y\}$, where X is the vector field $(\text{diag}x)(Ax + r)$ and Y is an additional
72 vector field associated to a specific treatment and to study the action of the pseudo-semigroup
73 $S(D)$ generated by concatenation of the positive orbits of the vectors fields denoted respec-
74 tively $\varphi_t = \exp tX$, $\psi_t = \exp tY$. The accessibility set at time t denoted $A(x_0, t)$ is the orbit
75 $S(D)(x_0)$ when the total time is t and its boundary contains the extremities of the time
76 minimal geodesics. It can be evaluated for small time using Lie brackets computations of X
77 and Y . This boundary can have a complicated structure but an intense research activities

78 at the end of the eighties was devoted to stratify this set under some suitable assumptions
79 in relation with the problem of computing a regular synthesis, see in particular [10], [12]. In
80 this research program the Maximum Principle [24] is a very powerful tool to analyze the op-
81 timal solutions since it gives a parametrization of the boundary of the accessibility set, where
82 the geodesics dynamics is the projection of an n -Hamiltonian dynamics that is a differential
83 system in dimension $2n$ and this system is not smooth.

84 Let us formulate this principle to analyze for instance the effect of an antibiotic or probiotic
85 treatment only, whence the control system takes the form

$$86 \quad \frac{dx}{dt}(t) = X(x(t)) + u(t)Y(x(t)),$$

87 where the control $u(\cdot)$ in the permanent case belongs to the set \mathcal{U} of bounded measurable
88 mappings valued in the convex set $U = [-1, +1]$, where $u = -1$ corresponds to zero dosing that
89 is $X - Y = (\text{diag}x)(Ax + r)$ while to maximal dosing corresponds the dynamics $(\text{diag}x)(Ax +$
90 $r) + 2Y(x)$, where $Y(x)$ is related to the action of the antibiotic or probiotic agent.

91 Consider the problem of reaching in minimum time a terminal manifold N related to reduce
92 the infected agent x_1 , e.g. reach a small population x_1 in minimal time (a dual formulation
93 of the problem is $\min x_1$ for fixed final time).

94 **Theorem 1.1.** *The Maximum Principle tells us that if $(x(\cdot), u(\cdot))$ is a time minimal control-*
95 *trajectory pair on $[0, t_f]$, then there exists a non vanishing adjoint n -dimensional vector $p(\cdot)$*
96 *such that the triple $(z(\cdot), u(\cdot))$, $z = (x, p)$ satisfies the equations that we introduce next.*

97 Denoting $H(z, u) := H_X(z) + uH_Y(z)$ the pseudo-Hamiltonian, where if Z is a vector field,
98 $H_Z(z) = p \cdot Z(x)$ denotes the Hamiltonian lift and M is the maximized or true Hamiltonian
99 $\max_{u \in [-1, +1]} H(z, u)$. Then for almost every t one has

$$100 \quad (1.2) \quad \frac{dx}{dt}(t) = \frac{\partial H}{\partial x}(x(t), p(t), u(t)), \quad \frac{dp}{dt}(t) = -\frac{\partial H}{\partial p}(x(t), p(t), u(t)).$$

101 Moreover the optimal control satisfies the maximization condition a.e.

$$102 \quad (1.3) \quad H(z(t), u(t)) = M(z(t)),$$

103 and M is a nonnegative constant.

104 At the terminal time t_f the transversality condition holds

$$105 \quad (1.4) \quad p(t_f) \perp T_{x(t_f)}^* N.$$

106 From the maximization condition one deduces that an optimal control is the concatenation
107 of:

- 108 • Regular subarcs where $u(t) = \text{sign}H_Y(z(t))$ a.e..
- 109 • Singular subarcs defined by the implicit relation $H_Y(z(t)) = 0$.

110 Such singular arcs define the geodesics solutions when relaxing the control bound to the whole
111 $u \in \mathbb{R}$. They form an Hamiltonian flow constrained to the switching set $\Sigma : H_Y(z) = 0$ in
112 which they filled in general a subset of codimension one. Hence they play an important role
113 in our study, see for instance the reference [4].

114 The main objective of this article is to analyze geometrically this dynamics in the case
115 of the controlled Lotka–Volterra equations and from the control optimal point of view it is
116 the analogue of the program of classifying the geometric dynamics for the Lotka–Volterra
117 model. The limit being essentially the same that is to handle the curse of dimension and the
118 computational complexity. Making the connection of the problem of minimizing the infection
119 with the problem of maximizing the production of one species for chemical network, our
120 objective is to use in this frame a series of articles started in the eighties, see for instance
121 [6, 21] in the frame of geometric optimal control [1, 4], aiming to optimize the production of
122 batch chemical reactors and recently pursued in [7].

123 Moreover in practice our objective is to compute an approximation of the time minimal
124 synthesis that is to reach the terminal manifold for every initial condition determining the
125 closed loop optimal control: $x \rightarrow u^*(x)$. Regularity conditions have to be satisfied in order
126 to define the solutions and they are related to the regularity properties of the time minimal
127 value function.

128 The article is organized as follows. In section 2 the controlled Lotka–Volterra model is
129 introduced and the optimal control problem presented in the frame of permanent controls.
130 The Maximum Principle leads to the classification of the geodesics in the context of geometric
131 optimal control and singularity theory using the seminal earliest contributions of [19, 20, 14].
132 The section 3 is based on the series of articles [6, 21, 7], dealing with a terminal manifold
133 of codimension one. They are rather technical and our contribution being to introduce two
134 main concepts. The first one is the notion of Whitney chart to determine in an appropriated
135 coordinates system the time minimal synthesis in a neighborhood of the terminal manifold
136 using the construction of semi-normal forms to estimate the switching and cut loci up to all
137 cases of codimension two for the C^∞ -Whitney topology. Secondly the concept of unfolding
138 from singularity theory is introduced in our control frame to reduce the classification to 2d and
139 3d cases and using their description (dictionary) of the aforementioned references. The final
140 section is devoted to the analysis and the classification of singular arcs in the 2d and 3d cases
141 to deduce the time minimal syntheses. In this program the computation can be automatized
142 in the 2d case using two classical invariants: the collinear set and the singular locus. In
143 dimension 3 the problem is intricate due to the complexity of the singular dynamics. But a
144 program of computations in the general case can be outlined based on gluing Whitney charts
145 as an alternative of programs as for example in [2] to derive patchy feedbacks to approximate
146 the time minimal function, our construction differing by the dominant use of the feedback
147 singular control.

148 2. Model of Controlled Lotka–Volterra Equation and Optimal Control.

149 **2.1. A quick tour in the 2d–Lotka–Volterra predator–prey model.** The original Lotka–
150 Volterra model analyzed in [28] describes, in the frame of (conservative) integrable dynamics,
151 the interaction between two species. More precisely it was constructed to explain the evo-
152 lution of the averaged populations of two fishing species in relation with diminution of the
153 fishing activity observed by D’Ancona during the first World War and succeeds to explain the
154 observation. From dynamical point of view it concerns the case of a center, the mechanical
155 analogue being the oscillating non linear pendulum and it was extended to the case of an
156 integrable saddle by Volterra himself. The limit of the model are clearly indicated in the

157 memoir and a parallel can be made with the $2d$ -reduced model of the gut microbiote that we
158 are analyzing in this paper.

159 We conserve the same notation than in the memoir. In the oscillatory situation the prey-
160 predator population $N = (N_1, N_2)$ satisfies the dynamics:

$$161 \quad (2.1) \quad \frac{dN_1}{dt} = N_1(\varepsilon_1 - \gamma_1 N_2), \quad \frac{dN_2}{dt} = -N_2(\varepsilon_2 - \gamma_2 N_1)$$

162 where $(\varepsilon_1, \varepsilon_2, \gamma_1, \gamma_2) > 0$, which can be written in a general form as

$$163 \quad (2.2) \quad \frac{dN_1}{dt} = N_1(\lambda_1 + \mu_1 N_2) \quad \frac{dN_2}{dt} = N_2(\lambda_2 + \mu_2 N_1)$$

164 for real parameters $\lambda_i, \mu_i, i = 1, 2$.

165 This leads to the equation

$$166 \quad (2.3) \quad \mu_2 \frac{dN_1}{dt} + \lambda_2 \frac{1}{N_1} \frac{dN_1}{dt} - \mu_1 \frac{dN_2}{dt} - \lambda_1 \frac{1}{N_2} \frac{dN_2}{dt} = 0$$

167 and integrating one gets

$$168 \quad \mu_2 N_1 + \lambda_2 \ln N_1 - (\mu_1 N_2 + \lambda_1 \ln N_2) = \text{constant.}$$

169 Hence

$$170 \quad N_1^{\lambda_2} e^{\mu_2 N_1} = C N_2^{\lambda_1} e^{\mu_1 N_2},$$

171 where C is a constant depending upon the initial conditions $(N_1(0), N_2(0))$.

172 Volterra describes the solution using the auxiliary curves

$$173 \quad (2.4) \quad Y = N_1^{-\varepsilon_2} e^{\gamma_2 N_1}, \quad X = N_1^{\varepsilon_1} e^{-\gamma_1 N_2}$$

174 so that the solution can be locally either represented as a graph $Y = CX$ or $X = CY$.

175 One denotes

$$176 \quad \Omega := (K_1, K_2) = \left(\frac{\varepsilon_2}{\gamma_2}, \frac{\varepsilon_1}{\gamma_1} \right)$$

177 the interior equilibrium.

178 Exact formulae give the time evolution of the population $t \mapsto N_i(t)$. But from physical point
179 of view, what matters is the averaged population $\langle N_i \rangle$ and a simple computation gives the
180 following.

181 **Theorem 2.1.** *The averaged populations are given by:*

$$182 \quad \langle N_i \rangle := \frac{1}{T} \int_0^T N_i(t) dt = K_i, i = 1, 2,$$

183 *which are not depending upon the initial conditions but only from the equilibrium Ω .*

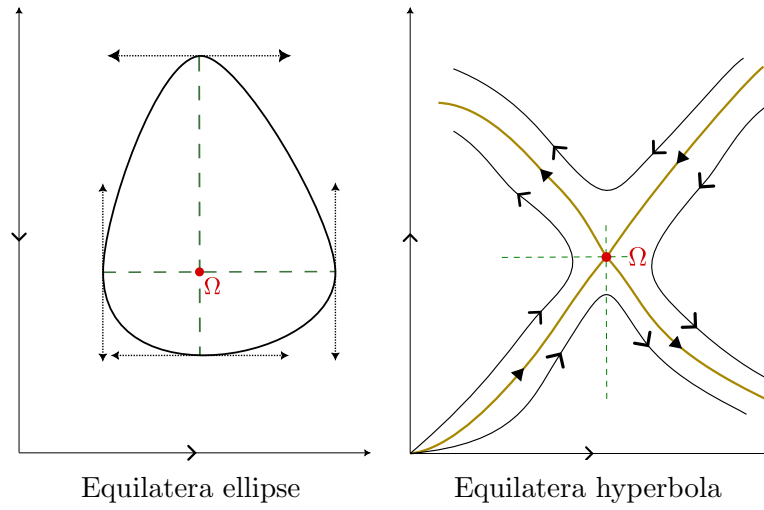


Figure 1. Volterra memoir. Left: center-case. Right: saddle case.

184 The Lotka–Volterra model can be normalized in the same category using the dimensionless
185 variables:

$$186 \quad n_1 := \frac{N_1}{K_1}, \quad n_2 := \frac{N_2}{K_2}$$

187 and we get

$$188 \quad (2.5) \quad \frac{dn_1}{dt} = \varepsilon_1 n_1 (1 - n_2), \quad \frac{dn_2}{dt} = -\varepsilon_2 n_2 (1 - n_1)$$

189 and the linearized system at Ω takes the form

$$190 \quad (2.6) \quad \frac{\delta n_1}{dt} = -\varepsilon_1 \delta n_2, \quad \frac{\delta n_2}{dt} = \varepsilon_2 \delta n_1.$$

191 The geometric construction of the dynamics in the memoir is based on the auxiliary curves
192 (2.4) to compute $Y = CX$.

193 This opens the path to treat in the same frame the case where $\varepsilon_1 \varepsilon_2 < 0$ so that Ω is a
194 saddle point to get the form $XY = C$. Volterra gives a geometric representation of the two
195 cases in a single figure, see Fig. 1.

196 Let us analyze in the oscillatory case the role of the fishing activity, introducing control
197 in the model. The system takes the form:

$$198 \quad (2.7) \quad \frac{dN_1}{dt} = (\varepsilon_1 - \alpha\lambda - \gamma_1 N_2)N_1, \quad \frac{dN_2}{dt} = -(\varepsilon_2 + \beta\lambda - \gamma_2 N_1)N_2,$$

199 where $\alpha, \beta \geq 0$ are the modes of destruction and $\lambda \geq 0$ is the intensity.

200 Assuming $\varepsilon_1 - \alpha\lambda > 0$ so that the population is still oscillating, the averaged values of
201 N_1, N_2 become

$$202 \quad \frac{\varepsilon_2 + \beta\lambda}{\gamma_2}, \frac{\varepsilon_1 - \alpha\lambda}{\gamma_1} \quad \text{versus} \quad \frac{\varepsilon_2}{\gamma_2}, \frac{\varepsilon_1}{\gamma_1}$$

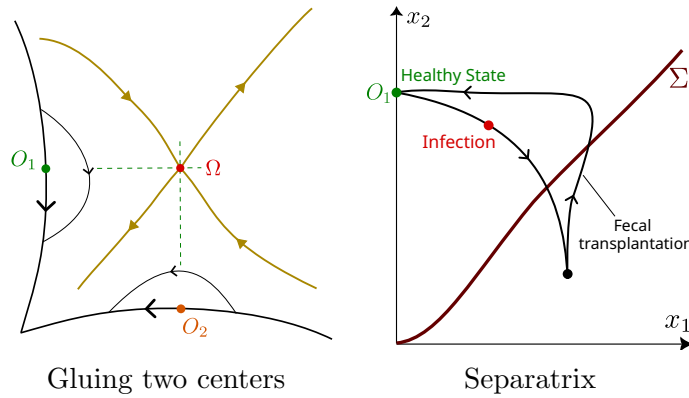


Figure 2. Jones et al. model .

203 without fishing activity (see Theorem 2.1). This confirms the observations by D’Ancona.

204 This simple model can be generalized to analyze, in the same frame, controlled populations
205 dynamics introducing dissipation in the model associated to non zero coupling coefficients, to
206 get a $2d$ -control model of the form

$$207 \quad (2.8) \quad \frac{dx}{dt} = (\text{diag}x) [(r + Ax) + u \epsilon],$$

208 where A is the interaction matrix, ϵ is the sensitivity vector and the control u is the intensity.

209 Hence, in this frame the role of the constant control $u = 1$ is to shift the interior equilibrium
210 and the spectrum of the linearized dynamics.

211 The previous discussion clarifies the construction by Jones et al. of a $2d$ -Lotka–Volterra
212 model to describe a complex microbiote with an interior saddle point and the interaction
213 between the *C. difficile* population x_1 and the healthy microbiote population aggregated into
214 a single population x_2 . Noting again $\Omega = (K_1, K_2)$ the interior saddle equilibrium and nor-
215 malizing: $x_1 \rightarrow \frac{x_1}{K_1}$, $x_2 \rightarrow \frac{x_2}{K_2}$, this leads to a system with four equilibria: Ω , the origin and
216 two non interior equilibria O_1, O_2 associated respectively to the reduced dynamics with x_1 or
217 x_2 equal zero. This can be interpreted as gluing together two prey-predators models (see Fig.
218 2).

219 The model simulates the following medical protocol:

$$220 \quad \begin{array}{ccccc} \text{day 0} & \longrightarrow & \text{day } k & \longrightarrow & \text{day } k' > k, \\ (\text{healthy mouse} & & (\text{C. difficile infection}) & & (\text{fecal transplantation}) \\ & & \& \text{antibiotic}), & \end{array}$$

221 where the control actions are the choice of the day of the transplantation and the composition
222 of the fecal injection.

223 The final state posterior to the fecal injection is either the healthy state O_1 or the infected
224 state O_2 .

225 A separatrix Σ is constructed in the $2d$ -model indicating the success or the failure of
226 the transplantation therapy. This yields decision algorithms based on the computations of the
227 parameters of the reduced models using the observations. The infection has to be compensated
228 by the fecal transplantation. The mathematical limit of the model being that each species

229 population shall satisfies $M \geq x_i \geq \varepsilon$, in particular if the x_2 population becomes too small
 230 the model is not valid. Also from medical point of view a probiotic injection versus antibiotic
 231 injection increases the healthy population aiming to struggle against infection.

232 **2.2. Controlled Lotka–Volterra model and optimal control.** Next we introduce the def-
 233 initions and concepts in a general frame.

234 **Definition 2.2.** Let $x = (x_1, \dots, x_n)^\top \in \mathbb{R}_+^n$ be the state of interacting species, x_1 being the
 235 infected agent, $x' = (x_2, \dots, x_n)^\top$ being the state of healthy agents. The dynamics is described
 236 by

$$237 \quad (2.9) \quad \frac{dx}{dt} = (\text{diag}x)(Ax + r)$$

238 the matrix $A = (a_{ij})$ being the matrix of coefficients of interaction and $r = (r_1, \dots, r_n)^\top$ is
 239 the vector of individual growth rate. We denote by $M^+ = \mathbb{R}_+^n$ the invariant domain $x_i > 0$
 240 and M^\sim the union of M^+ with its boundary. The dynamics is called regular if A is invertible.
 241 The interior equilibrium is the point $\Omega = (K_1, \dots, K_n)$ given by $x = -A^{-1}r$.

242 We note $n = (n_1, \dots, n_n)^\top$ the dimensionless coordinates so that Ω is identified to $(1, \dots,$
 243 $1)^\top$.

244 One can associate to (2.9) an hierarchy of dynamics replacing $x \rightarrow x' = (x_2, \dots, x_n)^\top$ and
 245 this leads to up to 2^n equilibria for the dynamics in the physical space, which can be easily
 246 computed by recurrence.

247 The dynamics can be compactified using Poincaré compactification, identifying \mathbb{R}^n to the
 248 hyperplane $(x, z = 1)$ in \mathbb{R}^{n+1} to define the system:

$$249 \quad \frac{dx}{dt} = (\text{diag}x)(Ax + r), \quad \frac{dz}{dt} = 0,$$

250 where the right-member can be homogenized to define an homogeneous vector field which can
 251 be projected on the n -sphere \mathcal{S}^n .

252 Each equilibrium of the hierarchy of dynamics can be classified according to the L -(linear)
 253 stability status associated to the linearized dynamics at equilibrium.

254 Our study is related to the interaction of k non interior equilibria interacting with the inte-
 255 rior equilibrium and one can introduce a model reduction consisting in a polynomial dynamics
 256 of the form: $\frac{dx}{dt} = P(x)$.

257 Introducing the ln-coordinates $x = e^y$ so that the system takes the form:

$$258 \quad (2.10) \quad \frac{dy}{dt} = (Ae^y + r),$$

259 where $y \in \ln M^+$ and the non interior equilibria are at the infinity.

260 We denote by $X(x)$ the vector field defined by (1.1) where x can be taken as the normalized
 261 coordinates.

262 **2.2.1. Antibiotic or probiotic agent.** For a single antibiotic or probiotic agent the control
 263 system takes the form

$$264 \quad (2.11) \quad \frac{dx}{dt} = X(x) + uY(x),$$

265 with $Y(x) = (\text{diag}x)(\varepsilon_1, \dots, \varepsilon_n)^\top$ is the sensitivity vector and the control $u(t)$ describes the
266 dosing regimen. Note that u can be restricted to domain $[0, 1]$ using normalizations.

267 This notation can be applied to the hierarchy of models so that this leads to an hierarchy
268 of control problems which can be analyzed independently. For instance, prior to infection one
269 can analyze the effect of probiotics agents where $\varepsilon_i > 0$, while posterior to infection one can
270 consider the effect of antibiotic treatment.

271 The set of admissible controls fits in the frame of permanent control, where $u(\cdot)$ is a
272 measurable mapping on $[0, t_f]$ valued in $[0, 1]$. Each measurable bounded mapping can be
273 approximated by a sequence of piecewise constant mappings in the L^∞ -topology and acces-
274 sibility can be studied restricting to this class. This is the point of view of geometric control
275 which leads to introduce the polysystem: $D = \{X + uY; u \text{ constant in the interval } [0, 1]\}$.

276 **2.2.2. Fecal transplantation and bactericide.** In the case of transplantation or bacteri-
277 cide the control system takes the form:

$$278 \quad \frac{dx}{dt} = X(x) + uY(x),$$

279 where $Y = (v_1, \dots, v_n)^\top$ is a constant vector field and u takes it values in the whole \mathbb{R}^+ , where
280 its action being to get Dirac pulse $\delta(t - t')$, defined as the limit of controls sequence: $u_n = \lambda n$
281 on $[t', t' + 1/n]$.

282 **2.2.3. Optimal control problem in the permanent case vs the sampled-data frame.**

283 Resuming the previous discussion, one can write the general control system in the form:

$$284 \quad \frac{dx}{dt}(t) = X(x(t)) + \sum_{\text{ant.,pro.}} u_i(t)Y_i(x(t)) + \sum_{\text{transp.,bac.}} u'_i(t)Y'_i(x(t)),$$

285 where the two sums are related respectively to probiotic, antibiotic agents and transplantations
286 and bactericides. Moreover discontinuity in the state $x = (x_1, \dots, x_n)^\top \rightarrow x' = (x'_1, x_2, \dots, x_n)^\top$
287 can be understood as the jump action $x \rightarrow x'$. Hence this leads in the general case to a mixture
288 of permanent and sampled-data control systems. The first action is related to permanent
289 control, but due to logistic medical constraints it can fit in the sampled-data frame, e.g. a
290 finite number of medical interventions at some predefined times: $0 < t_1 < \dots < t_k < t_f$ to
291 modify the treatment. The second action fits in the sampled-data frame, since in particular
292 it corresponds to invasive therapies.

293 In this article we concentrate to the permanent case associated to a single antibiotic or
294 probiotic agent.

295 **OCP in the permanent case.** The problem is either to reduce the x_1 -infection or to increase
296 the production or ratio of healthy agents, prior to infection. This leads to consider in a dual
297 formulation problems of the form:

- 298 • Reach in minimum time t_f a given terminal manifold N of codimension one for the
299 control system written as: $\frac{dx}{dt} = X(x) + uY(x)$, Y being associated to a specific
300 treatment.

301 In this formulation candidates as minimizers are selected using the Maximum Principle stated
302 in the introduction.

303 **2.3. Singular trajectories and time optimal control.** In this section, we make a brief
 304 recap of the properties of singular trajectories, crucial in our analysis, for full details see [4].

305 **Definition 2.3.** Let (X, Y) the pairs of C^ω (real analytic) vector fields on M associated to
 306 control system: $\frac{dx}{dt} = X(x) + uY(x)$. The feedback group G_f is the set of triples (φ, α, β) ,
 307 where φ is a local diffeomorphism and $u = \alpha(x) + \beta(x)v$, $\beta \neq 0$ is a feedback, the group
 308 structure being induced by the actions:

- 309 • local diffeomorphism $\varphi : (X, Y) \rightarrow (\varphi * X, \varphi * Y)$, where $\varphi * Z = d\varphi(Z \circ \varphi^{-1})$ denotes
 310 the image of a vector field Z .
- 311 • feedback: $u = \alpha(x) + \beta(x)v : (X, Y) \rightarrow (X + Y\alpha, Y\beta)$.

312 The control system can be lifted on the cotangent bundle T^*M with symplectic structure
 313 defined by $d\omega$, where $\omega = p dx$ is the Liouville form. The Hamiltonians $H_X(z) = p \cdot X(x)$,
 314 $H_Y(z) = p \cdot Y(x)$, where $z = (x, p)$ are the symplectic coordinates, are the Hamiltonian lifts
 315 of X, Y . The system lift takes the form: $\frac{dz}{dt} = \mathbf{H}_X(z) + u\mathbf{H}_Y(z)$, and $H_X(z) + uH_Y(z)$ is
 316 the pseudo or non maximized Hamiltonian. One can lift every local diffeomorphism φ into
 317 a Mathieu symplectomorphism φ defined by: $x = \varphi(y)$, $p = q \left(\frac{\partial \varphi}{\partial y} \right)^{-1}$, where p, q are row
 318 vectors. This induces an action of G_f on the pairs (H_X, H_Y) .

319 **2.3.1. Computations of singular extremals.** Relaxing the control bound to $u \in \mathbb{R}$, from
 320 the Maximum Principle the candidates as time minimizers are the so-called singular extremals
 321 control-trajectory pairs written shortly (z, u) solutions of the constrained Hamiltonian dyna-
 322 mics: $\frac{dz}{dt}(t) = \mathbf{H}(z(t))$, \mathbf{H} being the Hamiltonian vector field, the constraints coming from the
 323 maximization condition: $\frac{\partial H}{\partial u} = H_Y(z) = 0$.

324 Hence they are solutions contained in the switching set $\Sigma : H_Y(z(t)) = 0$. They can
 325 be computed, deriving this equation with respect to t . Introducing the Poisson bracket of
 326 $H_{Z_1}(z) = p \cdot Z_1(x)$, $H_{Z_2}(z) = p \cdot Z_2(x)$, by $\{H_{Z_1}, H_{Z_2}\}(z) = p \cdot [Z_1, Z_2](x)$.

327 Hence we deduce:

$$328 \quad (2.12) \quad \begin{aligned} H_Y(z(t)) &= \{H_Y, H_X\}(z(t)) = 0, \\ \{\{H_Y, H_X\}, H_X\}(z(t)) + u(t)\{\{H_Y, H_X\}, H_Y\}(z(t)) &= 0. \end{aligned}$$

329 We introduce the following.

330 **Definition 2.4.** The Generalized Legendre-Clebsch condition (GLC) along a singular ex-
 331 tremal $(z(\cdot), u(\cdot))$ on $(0, t_f]$ is given by:

$$332 \quad \frac{\partial}{\partial u} \frac{d^2}{dt^2} \frac{\partial H}{\partial u}(z(t)) = \{\{H_Y, H_X\}, H_Y\}(z(t)) \neq 0,$$

333 for every t in $[0, t_f]$. The switching surface is $\Sigma : H_Y(z) = 0$ and we denote Σ' the sub-
 334 set: $H_Y(z) = \{H_Y, H_X\}(z) = 0$. Then outside the collinear set of $Y(x)$ and $[Y, X](x)$, if
 335 $\{\{H_Y, H_X\}, H_Y\} \neq 0$, the restriction of the symplectic form $d\omega$ to Σ' defines a symplectic
 336 manifold $(M', \omega|_{M'})$.

337 This gives the following.

338 **Proposition 2.5.** Assume that the GLC-condition holds along $(z(t), u(t))$ then the extremal
 339 is called of minimal order. We have:

- 340 1. The singular control $u_s(\cdot)$ is the dynamic feedback: $u_s(z) = -\frac{\{\{H_Y, H_X\}, H_X\}(z)}{\{\{H_Y, H_X\}, H_Y\}(z)}$.
 341 2. Introduce the true Hamiltonian $H_s(z) := H_X(z) + u_s(z) H_Y(z)$, the singular extremals
 342 of minimal order are the solutions of $H_s(z)$ contained in the set Σ' .
 343 They are the solutions of $H_s(z)$ restricted to the symplectic manifold M' .

344 Higher-order singular extremals can be determined at any order using the following algo-
 345 rithm. If

$$346 \quad \{\{H_Y, H_X\}, H_Y\}(z(t)) = 0 \text{ and } \{\{H_Y, H_X\}, H_X\}(z(t)) = 0$$

347 then, deriving both relations one gets:

$$348 \quad \begin{aligned} & \{\{\{H_Y, H_X\}, H_Y\}, H_X\}(z(t)) + u(t) \{\{\{H_Y, H_X\}, H_Y\}, H_Y\}(z(t)) = 0, \\ & \{\{\{H_Y, H_X\}, H_X\}, H_X\}(z(t)) + u(t) \{\{\{H_Y, H_X\}, H_X\}, H_Y\}(z(t)) = 0. \end{aligned}$$

349 If the control cannot be derived from the previous equations, we repeat the derivation
 350 procedure.

351 2.3.2. Singular extremals as feedback invariants.

352 **Definition 2.6.** Let E, F be two vector spaces and G a group acting linearly on E, F . An
 353 homomorphism $\chi: G \rightarrow \mathbb{R} \setminus \{0\}$ is called a character. Let χ be a character, a semi-invariant
 354 of weight χ is a map $\lambda: E \rightarrow \mathbb{R}$ such that for all $x \in E, g \in G, \lambda(g \cdot x) = \chi(g)\lambda(x)$. It is called
 355 an invariant if $\chi = 1$. A map $\lambda: E \rightarrow F$ is a semi-covariant of weight χ if for all $x \in E,$
 356 $g \in G, \lambda(g \cdot x) = \chi(g)g \cdot \lambda(x)$. It is called a covariant if $\chi = 1$.

357 The following theorem is unveiled in [4, Theorem 13, p.103]

358 **Theorem 2.7.** Denote by λ_s the map which associates to the pair (X, Y) the Hamiltonian
 359 vector field H_s restricted to Σ' . Then it is a covariant for the respective actions of the feedback
 360 group. In particular singular extremals are feedback invariants.

361 2.3.3. High order Maximum Principle [18].

362 **Proposition 2.8.** Assume p is oriented using the convention of the Maximum Principle
 363 along the singular extremal $z(\cdot): H_X(z(t)) \geq 0$. Then a necessary time optimality condition
 364 on $]0, t_f]$ is given by

$$365 \quad \frac{\partial}{\partial u} \frac{d^2}{dt^2} \frac{\partial H}{\partial u}(z(t)) = \{\{H_Y, H_X\}, H_Y\}(z(t)) \geq 0.$$

366

367 **Definition 2.9.** The singular extremal $z(t) = (x(t), p(t)), t \in [0, t_f]$ is called strict if p is
 368 unique up to a scalar.

369 **Corollary 2.10.** Assume the strict case. Then the singular trajectories projections of sin-
 370 gular extremals of minimal order are stratified according to the following:

- 371 • Hyperbolic case: $H_X \cdot \{\{H_Y, H_X\}, H_Y\}(z) > 0,$
- 372 • Elliptic case: $H_X \cdot \{\{H_Y, H_X\}, H_Y\}(z) < 0,$
- 373 • Abnormal or exceptional case: $H_X(z) = 0.$

374 2.3.4. Applications.

375 **2d-case.** Singular extremals satisfy $H_Y = \{H_Y, H_X\} = 0$ so that singular trajecto-
 376 ries are located on the set \mathcal{S} : $\det(Y(x), [Y, X](x)) = 0$. Outside the collinear set \mathcal{C} :
 377 $\det(Y(x), X(x)) = 0$ one can takes Y, X as a frame and writing $[[Y, X], Y](x) = \alpha(x)X(x) +$
 378 $\beta(x)Y(x)$. The singular control is given by: $[[Y, X], X](x) + u_s(x) [[Y, X], Y](x) = 0$. Hyper-
 379 bolic case corresponds to $\alpha(x) > 0$ and elliptic case to $\alpha(x) < 0$.

380 **3d-case.** The 3d-case is already a very rich situation to analyze the singular extremals
 381 and the program goes as follows.

382 Introduce the following determinants:

$$383 \quad (2.13) \quad \begin{aligned} D(x) &= \det(Y(x), [Y, X](x), [[Y, X], Y](x)), \\ D'(x) &= \det(Y(x), [Y, X](x), [[Y, X], X](x)), \\ D''(x) &= \det(Y(x), [Y, X](x), X(x)), \end{aligned}$$

384 and using the relations

$$385 \quad (2.14) \quad \begin{aligned} H_Y(z) &= \{H_Y, H_X\}(z) = 0, \\ \{\{H_Y, H_X\}, H_X\}(z) + u_s \{\{H_Y, H_X\}, H_Y\}(z) &= 0, \end{aligned}$$

386 we can eliminate p and the singular control is given by the feedback:

$$387 \quad u_s(x) = -\frac{D'(x)}{D(x)}.$$

388

389 **Lemma 2.11.** *The action of the feedback group implies the following changes on D, D' and*
 390 *D'' :*

$$391 \quad D^{\phi^*X, \phi^*Y}(x) = \det\left(\frac{\partial\phi}{\partial x}\right) D^{X,Y}(\phi^{-1}(x)), \quad D^{X+\alpha Y, \beta Y}(x) = \beta^4 D^{X,Y}(x),$$

$$392 \quad D'^{\phi^*X, \phi^*Y}(x) = \det\left(\frac{\partial\phi}{\partial x}\right) D'^{X,Y}(\phi^{-1}(x)), \quad D'^{X+\alpha Y, \beta Y}(x) = \beta^3 \left(D'^{X,Y}(x) + \alpha D^{X,Y}(x)\right),$$

$$393 \quad D''^{\phi^*X, \phi^*Y}(x) = \det\left(\frac{\partial\phi}{\partial x}\right) D''^{X,Y}(\phi^{-1}(x)), \quad D''^{X+\alpha Y, \beta Y}(x) = \beta^2 D''^{X,Y}(x).$$

394 *In particular the surfaces $D = 0$ and $D'' = 0$ are feedback invariant.*

395 Defining the vector field:

$$396 \quad (2.15) \quad X_s(x) := X(x) + u_s(x)Y(x),$$

397 we have:

398 **Proposition 2.12.** *Singular trajectories of minimal order stratified the dynamics into:*

- 399 • *Hyperbolic arcs in $DD'' > 0$,*
- 400 • *Elliptic arcs in $DD'' < 0$,*
- 401 • *Exceptional or abnormal arcs in $D'' = 0$.*

402 From Lemma 2.11, we obtain the following proposition.

403 **Proposition 2.13.** *For the action of the feedback group $G_f = \{(\varphi, \alpha, \beta)\}$ reducing to φ -*
404 *changes of coordinates on vector fields X_s , the map $\lambda_s : (X, Y) \rightarrow X_s$ is a covariant. Hence*
405 *this allows to generate feedback invariants using the dynamics (2.15).*

406 Equilibria of this dynamics split into two types:

- 407 • If $D \neq 0$, they are given by the solutions of $X_s(x) = 0$.
- 408 • If $D = 0$, one can reparameterize the dynamics to get the vector field $D(x)X(x) -$
409 $D'(x)Y(x)$ and additional (non isolated) singular points are located on $D(x) = D'(x) =$
410 0 .

411 Exceptional trajectories are contained in the invariant set $D''(x) = 0$ for the dynamics.

412 3. Extremals classification and local time minimal syntheses near a terminal manifold 413 of codimension one.

414 **3.1. Introduction and definitions.** In this section we consider the time minimal con-
415 trol problem for the system: $\frac{dx}{dt} = X(x) + uY(x)$, $|u| \leq 1$, with terminal manifold N of
416 codimension one. We denote by $H(z, u) = H_X(z) + uH_Y(z)$ the pseudo-Hamiltonian and
417 $M(z) = \max_{|u| \leq 1} H(z, u)$ the true or maximized Hamiltonian. In this setting the control do-
418 main is taken as $U = [-1, +1]$, where extreme control values lead to introduce the vector fields
419 $X(x) - Y(x)$ (no medical treatment) or $X(x) + Y(x)$, that is the maximal dosing regimen.

420 **Definition 3.1.** *The extremals are concatenation of regular extremals for which almost eve-*
421 *rywhere*

$$422 \quad u(t) = \text{sign}H_Y(z(t))$$

423 *and singular extremals if*

$$424 \quad H_Y(z(t)) = 0$$

425 *holds identically.*

426 *An extremal is called exceptional if the maximized Hamiltonian is such that $M(z) = 0$.*
427 *A BC-extremal is an extremal satisfying the transversality condition. A switching time is*
428 *an instant such that the extremal control is discontinuous. A bang-bang extremal is a regular*
429 *extremal with a finite number of switches.*

430 Since the control domain is $U = [-1, +1]$, a singular extremal is called strictly feasible
431 (admissible) if $|u_s| < 1$ and saturating at time t if $|u_s(t)| = 1$. A regular or singular extremal is
432 called strict if p is unique up to a scalar. In the strict case singular extremals can be classified
433 into hyperbolic, elliptic and exceptional extremals. We denote by σ_+, σ_- bang arcs associated
434 respectively to $u = +1$ or $u = -1$, σ_s is a singular arc associated to u_s . We denote by $\sigma_1\sigma_2$
435 an arc σ_1 followed by σ_2 .

436 **Definition 3.2.** *Taking an open set V of M , the problem is called geodesically complete on*
437 *V if for each $x_0, x_1 \in V$ there exists a time minimizing geodesic in V joining x_0 to x_1 . Fixing*
438 *the target to $N (=N \cap V)$, a time minimal synthesis is a discontinuous feedback $x \rightarrow u^*(x)$ so*
439 *that the solutions of $\frac{dx}{dt} = X(x) + u^*(x)Y(x)$ are well defined and $u^*(x)$ is the optimal feedback*
440 *solution to steer x to the target in minimum time.*

441 **3.2. Small time classification of regular extremals.** In this section we recall some basic
 442 properties of regular extremals, see [19] but also [20] for the analysis of the Fuller phenomenon
 443 as a recommended reading.

444 The surface $\Sigma : H_Y(z) = 0$ is called the switching surface and we denote by Σ' the set
 445 $H_Y(z) = \{H_Y, H_X\}(z) = 0$. Let $z(\cdot) = (x(\cdot), p(\cdot))$ be a reference extremal on $[0, t_f]$. We note
 446 $\Phi(t) := H_Y(z(t))$ the switching function coding the switching times.

447 Deriving twice Φ with respect to time, one gets:

$$448 \quad \frac{d\Phi}{dt}(t) = \{H_Y, H_X\}(z(t)),$$

$$449 \quad (3.1) \quad \frac{d^2\Phi}{dt^2}(t) = \{\{H_Y, H_X\}, H_X\}(z(t)) + u(t)\{\{H_Y, H_X\}, H_Y\}(z(t)).$$

450 **Definition 3.3.** *The time t is called an ordinary switching time if $\Phi(t) = 0$ and $\frac{d\Phi}{dt}(t) \neq$*
 451 *0.*

452 **Lemma 3.4.** *Assume t be an ordinary switching time, then near $z(t)$ every extremal projects*
 453 *onto:*

- 454 • $\sigma_+\sigma_-$ if $\frac{d\Phi}{dt}(t) > 0$,
- 455 • $\sigma_-\sigma_+$ if $\frac{d\Phi}{dt}(t) < 0$.

456 **Definition 3.5.** *Let $z(\cdot)$ be a bang extremal on $[0, t_f]$ with $u = \varepsilon \in \{-1, +1\}$. We note*
 457 *by $\frac{d^2\Phi_\varepsilon}{dt^2}$ the expression (3.1) in which $u \equiv \varepsilon$. The point $z(t)$ is called a fold point if $\Phi(t) =$*
 458 *$\frac{d\Phi}{dt}(t) = 0$ and $\frac{d^2\Phi_\varepsilon}{dt^2}(t) \neq 0$. Assume that Σ' is a regular surface of codimension two. We have*
 459 *three cases:*

- 460 • *Parabolic case:* $\frac{d^2\Phi_+}{dt^2}(t) \frac{d^2\Phi_-}{dt^2}(t) > 0$,
- 461 • *Hyperbolic case:* $\frac{d^2\Phi_+}{dt^2}(t) > 0$ and $\frac{d^2\Phi_-}{dt^2}(t) < 0$,
- 462 • *Elliptic case:* $\frac{d^2\Phi_+}{dt^2}(t) < 0$ and $\frac{d^2\Phi_-}{dt^2}(t) > 0$.

463 This leads to:

464 **Proposition 3.6.** *In the neighborhood of a fold point every extremal projects onto:*

- 465 • *In the parabolic case:* $\sigma_+\sigma_-\sigma_+$ or $\sigma_-\sigma_+\sigma_-$.
- 466 • *In the hyperbolic case* $\sigma_\pm\sigma_s\sigma_\pm$.
- 467 • *In the elliptic case, every extremal is bang-bang but the number of switches is not*
 468 *uniformly bounded.*

469 This is illustrated in Fig. 3.

470 Note that in the elliptic case, there is a foliation by a cylinder of the regular extremal dyna-
 471 mics and the number of switches is related to the distance to Σ' versus the Fuller phenomenon,
 472 where the sequence of regular arcs is not bang-bang and converges to Σ' .

473 **Application to the 3d–case.** Consider the case where Y , $[Y, X]$ and X form a frame i.e.

$$474 \quad D'' = \det(Y, [Y, X], X)$$

475 is not vanishing. The problem is strict for singular extremals since Y and $[Y, X]$ are indepen-
 476 dent. Hyperbolic trajectories are small time minimizing trajectories, while elliptic trajectories

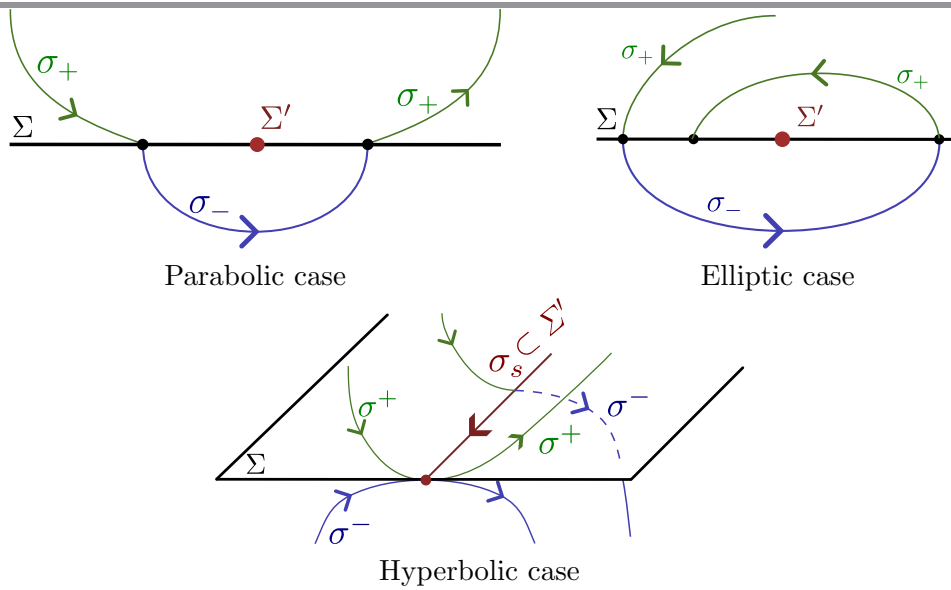


Figure 3. Fold case.

477 are small time maximizing, this up to the first conjugate time t_{1c} computed in [5] if they are
 478 strictly admissible (even in the limit case with no constraints on the control). In the parabolic
 479 case, they can be absent or not feasible. Consider the separating case where the singular arc
 480 is exceptional (abnormal) and assume that it is strictly admissible (for instance relaxing the
 481 control bound to the whole \mathbb{R}). In this case using again [5] an exceptional arc σ_s is time
 482 minimizing and time maximizing, up to the first conjugate time t_{1c} . Such a point is absent in
 483 the $3d$ -case. Such an arc can be lifted into two extremals $(\pm p, \sigma_s)$ and it corresponds either
 484 to an hyperbolic or elliptic situation in Σ' . One contribution of [21] is to analyze the time
 485 minimal syntheses near the terminal manifold in this situation.

486 **3.3. General concepts of regular synthesis with a terminal manifold of codimension**
 487 **one.** Take a triple (X, Y, N) and let $x_0 \in N$ which can be identified to 0 while N is the plane
 488 $x_1 = 0$. Let U be a neighborhood of 0, which divides the space into neighborhoods V and W
 489 contained respectively in $x_1 < 0$ and $x_1 > 0$ so that $U = V \cup W$. The problem is to compute
 490 the time minimal regular synthesis to steer each point of U to the terminal manifold.

491 N can be taken locally as $f^{-1}(0)$ where f is a submersion from U into a neighborhood of
 492 0 in \mathbb{R} . The set of triples (X, Y, f) is endowed with the C^∞ -Whitney topology and we denote
 493 by $j^k X$ (resp. $j^k Y, j^k f$) the k -jet of X (resp. Y, f) obtained by taking the Taylor expansion
 494 at $x_0 = 0$ up to order k . We say that the triple (X, Y, f) has at 0 a singularity of codimension
 495 i if $(j^k X, j^k Y, j^k f)$ belongs to a semi-algebraic set of codimension i in the jet space.

496 Our aim is to make a short presentation of the results of [6, 21, 7] to classify local syn-
 497 theses up to an homeomorphism preserving the target N for all cases of codimension ≤ 2 , by
 498 considering two cases occurring in the application that we introduce next.

499 **Definition 3.7.** When Y is everywhere tangent to the target N , the control u is indirect and
 500 this case is called the flat case. In the non flat case, the action of the control is direct and the

501 set of points where Y is tangent to N is of codimension ≥ 1 .

502 **3.3.1. Stratified synthesis.** Our aim is to describe the local time minimal synthesis in
 503 a neighborhood of N by estimating at any order the different strata. Actually, the optimal
 504 control feedback $u^*(x)$ is not always defined on the whole subset V of U in the domain $x_1 < 0$
 505 , since for some $x \in V$ the target N is not accessible.

506 In fact we can reduce our study to two cases:

- 507 • The case when the convex cone C generated by $\{X \pm Y\}$ is strict and the set of
 508 admissible directions points towards the space $x_1 > 0$.
- 509 • The exceptional case where the set of admissible directions are tangent to the terminal
 510 manifold.

511 This leads to introduce the exceptional locus in the construction of the stratification of N .

512 **Definition 3.8.** Let n be the normal to N oriented toward $x_1 > 0$. The exceptional locus
 513 (restricted to N) \mathcal{E} is the set of points of N such that: $n(x) \cdot Y(x) = n(x) \cdot X(x) = 0$.

514 The second part of the stratification amounts to introduce the singular locus.

515 **Definition 3.9.** The singular locus (restricted to N) \mathcal{S} is the set of points of N such that:
 516 $n(x) \cdot Y(x) = n(x) \cdot [Y, X](x) = 0$.

517 **Definition 3.10.** A stratified synthesis amounts to find a partition of V (or a partition of
 518 U in the exceptional case) into V^+ (resp. U^+) where $u^*(x) = +1$ and V^- (resp. U^-) where
 519 $u^*(x) = -1$ and a stratified surface separating V^+ and V^- (resp. U^+, U^-) with three kind of
 520 strata:

- 521 • *Switching locus.* It is the closure of the set of ordinary switching points and forming
 522 the set W_{\sharp} , $\sharp \in \{-1, +1\}$, where W_+ is associated to $\sigma_+\sigma_-$ and W_- to $\sigma_-\sigma_+$.
- 523 • *Cut locus.* Let $\sigma : [t_f, 0] \rightarrow M$ be a minimizing curve, integrating backwards from N so
 524 that $\sigma(0) \in N, t_f < 0$. The cut-locus is the closure of the set of points where optimality
 525 is lost. It is denoted C and contains the splitting locus L where the optimal feedback
 526 is not unique.
- 527 • *Switching singular locus.* It is foliated by optimal singular arcs and is denoted Γ_s .
 528 Recall that if $u_s \in]-1, +1[$ the singular arc is strictly feasible but it can be saturated
 529 if $u_s^*(x) \in \{-1, +1\}$.

530 To estimate the different strata we use semi-normal forms restricting the action of the feedback
 531 group to local diffeomorphisms φ preserving 0 and feedbacks $u \rightarrow -u$ so that σ_+ and σ_- can
 532 be inverted in the classification.

533 We can choose local coordinates to normalize a reference trajectory to $t \mapsto (t, 0, \dots, 0)$,
 534 the terminal manifold N and the controlled vector field Y to compute the optimal synthesis
 535 in a neighborhood of N . More precisely, we introduce the following important concept.

536 **Definition 3.11.** Let $x_0 \in N$ which can be identified to 0. A Whitney chart is a pair (U, φ)
 537 where U is a neighborhood of x_0 and φ a system of coordinates $(x, y, y_1, \dots, y_{n-3}, z)$ such that:

- 538 1. $Y = \frac{\partial}{\partial z}$,
- 539 2. N is the surface of codimension one parameterized by $(ks^2 + s^2O(|w_1, w_2, \dots, w_{n-3},$
 540 $w, s|), w, w_1, \dots, w_{n-3}, s)$,
- 541 3. The time minimal synthesis in U is C^0 described with foliations by 2d or 3d syntheses

542 with triples $(X^b(x), Y^b(x), N^b(x))$, $x \in \mathbb{R}^2$ or \mathbb{R}^3 where the 3d-cases occur only in the
543 exceptional case if $n \geq 3$.

544 Moreover in U , one can construct the stratified optimal synthesis, where each strata can be
545 estimated at any order.

546 **Definition 3.12.** In the previous construction the restriction from n to $n - 1$ decomposing
547 $x = (x', \lambda)$, $N = \cup_{\lambda} N'(\lambda)$, where $\lambda \in \mathbb{R}$, is a parameter is called a one dimensional unfolding.

548 The previous definitions will be clarified in the examples we present next.

549 **3.3.2. Main points of the geometric and analytic construction.** One can restrict our
550 presentation to the 2d-case. Let $n(x)$ be the normal to N , oriented towards $x_1 > 0$. We
551 denote by N^\perp the symplectic lift of N : $N^\perp = \{(x, p); x \in N, p = n(x)\}$. The stratification
552 of N by the conditions $n(x) \cdot Y(x) = 0$ and $n(x) \cdot [Y, X](x) = 0$ selects ordinary switching
553 points or fold points classified in Proposition 3.6.

- 554 • Ordinary switching locus K : One can restrict for simplicity the analysis to the 2d non
555 flat case. Let $x_0 \in N$ such that $n \cdot Y(x_0) = 0$ and both $n \cdot X(x_0)$ and $n \cdot [Y, X](x_0)$ non
556 zero. This leads to compute a switching locus K terminating at x_0 . Such a switching
557 locus is part of W if the corresponding bang-bang extremal crosses the switching locus
558 versus reflects on the switching locus. This leads to estimate the slope of K .
- 559 • Singular locus Γ_s : Consider again the non flat case. Let x_0 such that $(n(x_0), x_0)$ is a
560 fold point hence $n \cdot Y(x_0) = n \cdot [Y, X](x_0) = 0$. Moreover assume that $n \cdot X(x_0) \neq 0$
561 (non exceptional case) and that the singular arc σ_s terminating at x_0 is strictly ad-
562 missible, such an arc being small time minimizing for the problem with fixed extrem-
563 ities (assuming the condition $n \cdot [[Y, X], Y](x_0) \neq 0$). One can choose coordinates
564 (x, y) such that $Y = \frac{\partial}{\partial y}$ and N is given by $(\frac{1}{2}ks^2, s)$, while X can be normalized to
565 $(1 - y^2 X_1(x, y)) \frac{\partial}{\partial x} + (u - u_s(x) + y X_2(x, y)) \frac{\partial}{\partial y}$, where σ_s is identified to $t \rightarrow (t, 0)$
566 and u_s is the singular control. Note that such normalizations were introduced in [5]
567 in a more general context.

568 In order to decide about optimality one can compare by direct computations in the normalized
569 coordinates the curvature of the boundary of the accessibility set along the singular arc with
570 the curvature of N given by k . This leads to the cases described in Fig. 4. In the first case,
571 there exists a cut locus C with slope $-u_s(0)$.

572 The 3d-case with an hyperbolic point terminating at $x_0 = 0$ can be obtained by construct-
573 ing a semi-normal form in coordinates (x, y, z) by unfolding the case $k > 0$ and this leads to
574 Fig. 5.

575 The central picture corresponds to Fig. 4 with $k > 0$. Left we have represented a Whitney
576 neighborhood containing the optimal switching locus W_+ intersecting the hyperbolic singular
577 locus. They can be easily computed using the stratification of N^\perp into sectors with ordinary
578 switching points and fold points while the singular arc terminating at 0 corresponds to an
579 hyperbolic fold point.

580 This gives the procedure to compute the optimal syntheses using [6] in the non exceptional
581 case as unfolding of 2d-cases. The procedure fails in the exceptional case for $n \geq 3$, where
582 the following example from [21] shows why it cannot be reduced to 2d-foliations.

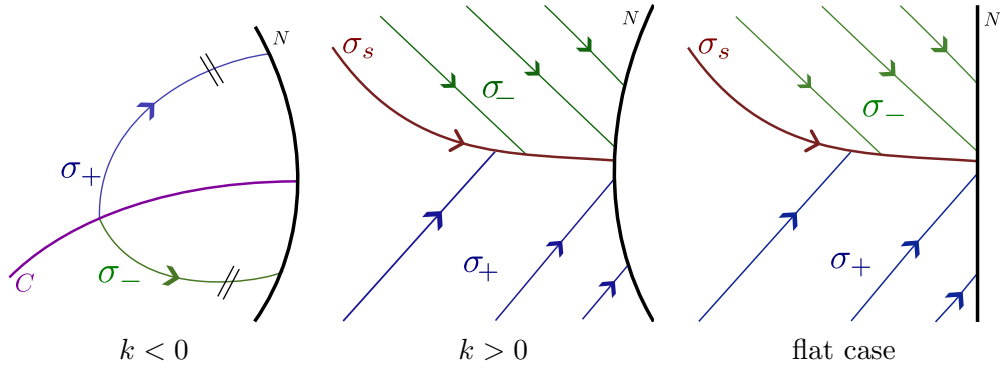


Figure 4. Optimal synthesis in the 2d-hyperbolic case.

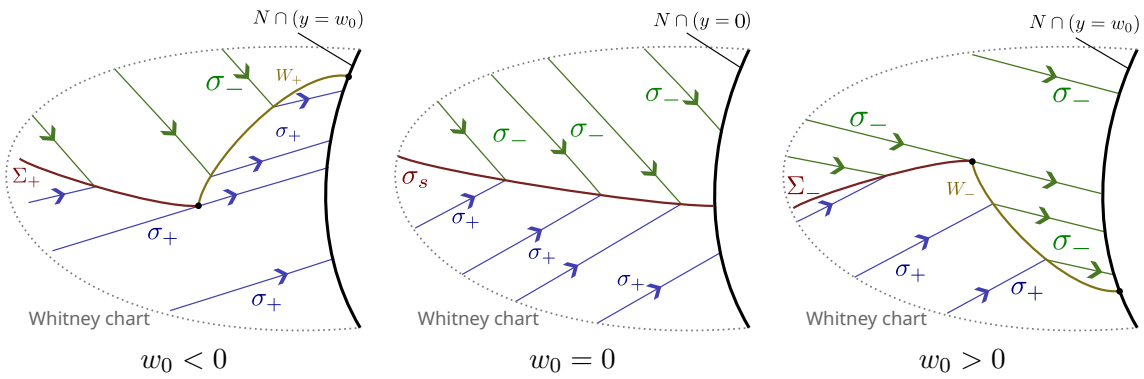


Figure 5. Unfolding in the 2d-hyperbolic case with parameter w_0 .

583 **3.3.3. An exceptional 3d–case not 2d–reducible.** One take a flat case so that N can be
 584 identified to $(0, w, s)$ in (x, y, z) coordinates and $Y = \frac{\partial}{\partial z}$. In the construction the main point
 585 is to take a bang arc σ_- , which is optimal in the domain $x \geq 0$ with a contact of order 3 at 0
 586 with the surface N . Hence this gives birth in the domain $x > 0$ to arcs σ_- intersecting three
 587 times the target N , thanks to contact analysis.

588 Such a situation occurs for instance for the model which in fine is a C^0 –normal form
 589 describing the situation:

590
$$\frac{dx}{dt} = z, \quad \frac{dy}{dt} = b, \quad \frac{dz}{dt} = 1 + u + y,$$

591 the target N given by $(w, s) \rightarrow (0, w, s)$.

592 One considers the situation with $b > 0$, where each point of the neighborhood U can be
 593 steered to the target.

594 In the domain $x < 0$, every time optimal trajectory is of the form σ_+ and the contact of
 595 σ_+ at 0 with N is of order 2.

596 Optimal arcs $\sigma_-(t)$ included in $x \geq 0$ are satisfying:

597 (3.2)
$$x_-(t) = t(s + wt/2 + bt^2/6 + \dots),$$

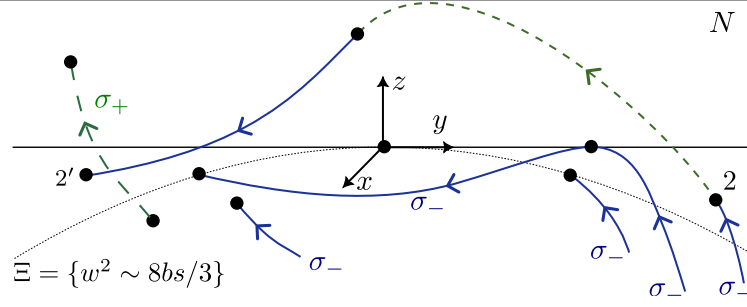


Figure 6. Synthesis exceptional case when $b < 0$. σ_- has a contact of order 3 with N .

598 where the weight of s is one and the weight of w is two, neglected having weights greater than
599 3.

600 The curve Ξ is the set of points $(0, w, s)$ of N such that: $\frac{x_-(t)}{t} = \frac{d}{dt} \left(\frac{x_-(t)}{t} \right)$ have a common
601 zero and is given using (3.2) by: $w^2 \sim \frac{8bs}{3}$.

602 The optimal synthesis is represented on Fig. 6. Optimal arcs σ_- in the domain $x \geq 0$ are
603 cutting twice N in the subsets of the target denoted 2 and 2' and have two subarcs which are
604 optimal in $x > 0$, but the subarc in $x < 0$ is not optimal.

605 **4. Computations and preliminary results on the Controlled Lotka–Volterra model.** The
606 aim of this section is to present the geometric study of the controlled Lotka–Volterra model:

607
$$\frac{dx}{dt}(t) = X(x(t)) + u(t)Y(x(t)),$$

608 with $X(x) = (\text{diag } x)(Ax + r)$ and $Y(x) = (\text{diag } x)\epsilon$, where $x = (x_1, \dots, x_n)^T$ is the population
609 species, x_1 represents the infected species and $\epsilon = (\epsilon_1, \dots, \epsilon_n)^T$.

610 The system can be written in ln-coordinates: $y = \ln x$ and it takes the form:

611 (4.1)
$$\frac{dy}{dt} = (Ae^y + r) + u\epsilon.$$

612 **4.1. Equilibria and the collinear set.** The collinear set \mathcal{C} is one of the main feedback in-
613 variant, related to computations of the free equilibria of the system for the hierarchy of models
614 with no treatment $u = 0$ or maximal dosing treatment $u = 1$, but also for all intermediate
615 dosing.

616 This set is a one dimensional algebraic variety and is the projection of the set:

617 (4.2)
$$\{(x_e, u_e) \in \mathbf{R}^n \times \mathbb{R}; \exists u_e, X(x_e) + u_e Y(x_e) = 0\}.$$

618 At such a point introduce the Jacobian matrix:

619
$$J(x_e, u_e) = \frac{\partial}{\partial x|_{(x_e, u_e)}} (X(x) + u_e Y(x)).$$

620 The following dimensionless coordinates are useful in the computations.

621 The system can be written:

$$622 \quad (4.3) \quad \frac{dx_i}{dt} = x_i r_i - x_i \sum_{j=1}^n a_{ij} x_j + u x_i \varepsilon_i$$

623 and denotes by x^* the free equilibrium given by:

$$624 \quad r_i - \sum_{j=1}^n a_{ij} x_j^* = 0, i = 1, \dots, n.$$

625 One sets $v_i = \frac{x_i}{x_i^*}$ so that the dynamics takes the form:

$$626 \quad \frac{dv_i}{dt} = v_i r_i - v_i \sum_{j=1}^n a_{ij} x_j^* v_j + u v_i \varepsilon_i,$$

627 and denoting $a_{ij}^* = a_{ij} x_j^*$, one has $r_i = \sum_{j=1}^n a_{ij}^*$ since the interior equilibrium is normalized
628 to $\Omega = (1, \dots, 1)$.

629 If we set: $x_i = v_i - 1$, the dynamics is given by:

$$630 \quad \frac{dx_i}{dt} = (x_i + 1) \sum_{j=1}^n a_{ij}^* - (x_i + 1) \sum_{j=1}^n a_{ij}^* (x_j + 1) + u (x_i + 1) \varepsilon_i.$$

631 Hence we have:

632 **Proposition 4.1.** *In the dimensionless coordinates the controlled Lotka–Volterra model is*
633 *given:*

$$634 \quad \frac{dx_i}{dt} = -(x_i + 1) \sum_{j=1}^n a_{ij} x_j + u (x_i + 1) \varepsilon_i,$$

635 so that Ω is identified to 0 and the Jacobian matrix at 0 is $-A$.

636 **4.1.1. Computations in the 2d–case in the dimensionless coordinates.** We consider the
637 regular 2-dimensional dynamics given in Proposition 4.1.

638 **Collinear set and classification of equilibria.** The collinear set is one of the main feedback
639 invariant related to the computations of free equilibria with no treatment $u = 0$ and forced
640 equilibria with maximal dosing $u = 1$.

641 The collinear set is given by the determinantal variety: $\det(X(x), Y(x)) = 0$:

$$642 \quad (x_1 + 1)(x_2 + 1)(x_1 \kappa_2 - x_2 \kappa_1) = 0,$$

643 where $\kappa_1 = \varepsilon_1 a_{22} - \varepsilon_2 a_{12}$ and $\kappa_2 = \varepsilon_2 a_{11} - \varepsilon_1 a_{21}$.

644 Alternatively, it can be viewed as the one dimensional algebraic variety projection of the
645 set

$$646 \quad \{(x, u_e) \in \mathbb{R}^2 \times \mathbb{R}, \exists u_e \text{ such that } X(x) + u_e Y(x) = 0\}.$$

647 The condition $u_e \in [0, 1]$ selects a segment of persistent equilibria located on the line:

$$648 \quad \mathcal{C} := \left\{ x_2 = u_e(x_1) \frac{\kappa_2}{\det A}, u_e(x_1) = x_1 \frac{\det A}{\kappa_1} \in [0, 1] \right\}.$$

649 In particular, introduce $x_e = (x_{1e}, x_{2e}) \in \mathcal{C}$, the origin $x_e = 0$ is associated to the control
650 $u_e = 0$ while $x_e = (\kappa_1/\det A, \kappa_2/\det A)$ is associated to the control $u_e = 1$.

651 For $u_e \in [0, 1]$, define the Jacobian matrix

$$652 \quad J(x_e, u_e) = \frac{\partial}{\partial x} (X(x) + u_e Y(x))|_{x=x_e},$$

653 we have:

654 **Lemma 4.2.** *Let $x_e \in \mathcal{C}$ associated to the control u_e , the spectrum of J is:*

$$655 \quad \text{spec}(J(x_e, u_e)) = \left\{ \left(k(x_e) \pm \sqrt{k(x_e)^2 + k'(x_e)} \right) / 2 \right\},$$

656 where $k(x) = -x_1 a_{22} \kappa_2 / \kappa_1 - a_{22} - a_{11}(x_1 + 1)$ and $k'(x) = -4 \det A (x_1 + 1) (1 + x_1 \kappa_2 / \kappa_1)$.

657 **4.2. Computation of the collinearity locus and properties. Construction of a normal**
658 **form in \ln -coordinates.**

659 **Computations about \mathcal{C} in the n -dimensional case.** We have the following algorithm,
660 taking the system represented in the x -coordinates.

- 661 • Step 1. The collinear set is the projection of the algebraic curve defined by: There
662 exists u_e constant such that $X(x_e) = -u_e Y(x_e)$. This gives n -equations depending
663 upon $(n + 1)$ variables (x_e, u_e) .
- 664 • Step 2. Take such a pair (x_e, u_e) so that x_e is a forced equilibrium for $u = u_e$ and they
665 form a set with extreme points associated to $u_e = 0$ and $u_e = 1$, when restricting to
666 $u_e \in [0, 1]$.

667 The linear dynamics at the point x_e is characterized by the Jacobian matrix:

$$668 \quad J(x_e, u_e) = \frac{\partial}{\partial x}|_{(x_e, u_e)} (X(x) + u_e Y(x))$$

669 the spectrum being $\sigma(J) = (\lambda_1, \dots, \lambda_n)$ with associated generalized eigenspaces $E_{\lambda_i}, i =$
670 $1, \dots, n$.

671 The linear stability is determined by this spectrum, thanks to Lyapunov linear stability
672 theory.

673 • Step 3. From control point of view we have three cases:

- 674 1. $u_e \notin [0, 1]$: u_e is not feasible,
- 675 2. $u_e \in]0, 1[$: u_e is strictly feasible,
- 676 3. $u_e = \pm 1$: u_e being feasible but saturating.

677 One can discuss the linear controllability of the pair $(J(x_e, u_e), b)$ where $b = Y(x_e)$.

- 678 • Kalman condition: $\text{rank} [b, Jb, \dots, J^{n-1}b] = n$ and the singular point x_e is regular. If
679 the control u_e is strictly feasible local controllability holds [22].

680 • If $\text{rank}[b, Jb, \dots, J^{n-1}b] = n - k < n$, then the singular point is a singular trajectory
 681 (reduced to a point) associated to u_e and k is the codimension of the singularity.

682 From linear controllability theory, one can construct a normal form, at a given equilibrium
 683 pair (x_e, u_e) .

684 We take ln-coordinates so that $X(x)$ takes the form $X^b(y) = (Ae^y + r)$ and the controlled
 685 vector field $Y(x)$ becomes the constant vector field $Y^b = \epsilon$.

686 Let (y_e, u_e) be the selected forced equilibrium in the ln-coordinates and let $z = y - y_e$,
 687 $v = (u - u_e)$ so that the system takes the form:

$$688 \quad \frac{dz}{dt} = J(z) + R(z) + v\epsilon,$$

689 where J is the Jacobian matrix at (y_e, u_e) .

690 One can find coordinates such that the linear dynamics decomposes into

$$691 \quad \begin{aligned} \frac{dz_1}{dt} &= J_{11}z_1 + J_{12}z_2 + v\epsilon \\ \frac{dz_2}{dt} &= J_{21}z_2 \end{aligned}$$

692 where the restriction to the controllable space $z_2 = 0$ is given by the dynamics:

$$693 \quad \frac{dz_1}{dt} = J_{11}z_1 + v\epsilon.$$

694 The pair (J_{11}, ϵ) can be set in Brunovsky canonical form:

$$695 \quad J_{11} = \left[\begin{array}{c|ccc} 0 & & & \\ \hline & \text{Id}_{n-k-1} & & \\ \hline -a_1 & -a_2 & \dots & -a_{n-k} \end{array} \right], \quad \epsilon = \begin{bmatrix} 0 \\ \vdots \\ 0 \\ 1 \end{bmatrix},$$

696 where the coefficients (a_1, \dots, a_{n-k}) are the coefficients of the characteristic polynomial of
 697 J_{11} .

698 Finally this leads to the construction of a normal form:

$$699 \quad \frac{dz}{dt} = J(z) + R(z) + v\epsilon,$$

700 where the pair $(J(x_e), u_e), \epsilon$ is in linear canonical form. Note in particular that the sensitivity
 701 vector ϵ is normalized to $(0, \dots, 0, 1)^T$ and $R(z)$ is the non linear part of the dynamics, related
 702 to singular trajectories computations.

703 **4.3. Singular extremals.** Lie brackets can be computed in the original coordinates but
 704 the computations are simpler in ln-coordinates, since the control vector field Y^b is constant.
 705 This comes from the following.

706 **Proposition 4.3.**

- 707 1. If $X = (\text{diag}x)X_1(x)$, $Y = (\text{diag}x)Y_1(x)$, where X_1, Y_1 are polynomic then the ite-
708 rated Lie brackets are in the same category of polynomic vector fields of the form
709 $(\text{diag}x)P(x)$.
710 2. Let φ be the diffeomorphism: $x = e^y$. Denote by X^b, Y^b the images of X, Y by this
711 diffeomorphism. Then by invariance of the Lie bracket: $[X^b, Y^b](y) = d\varphi^{-1}[X, Y](e^y)$.

712 **4.3.1. Computations in the 2d–case.** We start by computing the ln–coordinates:

- 713 • $X^b = \left(r_1 + \sum_{j=1,2} a_{1j}e^{x_j}, r_2 + \sum_{j=1,2} a_{2j}e^{x_j} \right)$,
714 • $Y^b = (\varepsilon_1, \varepsilon_2)$,
715 • $[X^b, Y^b] = \left(\sum_{j=1,2} \varepsilon_j a_{1j}e^{x_j}, \sum_{j=1,2} \varepsilon_j a_{2j}e^{x_j} \right)$.

716 Hence the singular locus: $\mathcal{S} : \det([X, Y](x), Y(x)) = 0$ is given by:

717 (4.4)
$$x_1x_2 (\varepsilon_1x_1\kappa_2 - \varepsilon_2x_2\kappa_1) = 0$$

718 which is stratified into $x_1 = x_2 = 0$ and a permanent straight-line $L : \varepsilon_1x_1\kappa_2 = \varepsilon_2x_2\kappa_1$.

719 Moreover:

- 720 • $[[X^b, Y^b], Y^b] = \left(\sum_{j=1,2} \varepsilon_j^2 a_{1j}e^{x_j}, \sum_{j=1,2} \varepsilon_j^2 a_{2j}e^{x_j} \right)$.

721 Outside the collinear set \mathcal{C} , X, Y form a frame and writing:

722
$$[[Y, X], X](x) = \alpha(x)X(x) + \beta(x)Y(x),$$

723 so that:

- 724 • Hyperbolic (feasible) subarcs are such that $\alpha(x) > 0$,
725 • Elliptic subarcs are such that $\alpha(x) < 0$.
726 • At the persistent point intersection of \mathcal{S} and \mathcal{C} , one gets an exceptional point.

727 **4.3.2. Computations in the 3d–case.** The Lie brackets computations are as before, ex-
728 cept that the index j goes from 1 to 3. So that

729
$$D = \det(Y^b, [Y^b, X^b], [[Y^b, X^b], Y^b])$$

730 is homogeneous and quadratic with respect to the variable e^{x_i} .

731 Moreover the exceptional locus is given by the relation:

732
$$D'' = \det(Y^b, [Y, X]^b, X^b) = 0,$$

733 this set being a quadratic non homogeneous variety with respect to the variables e^{x_i} .

734 Note that the computation of the Lie bracket: $[[Y^b, X^b], X^b]$ is more complex and formal
735 computations are necessary.

736 This fixes the limit of the computational complexity in the n –dimensional case.

737 4.4. Applications.

738 **4.4.1. A 2d–working case.** In this section, the general techniques from [6, 21] will be
739 applied to analyze a 2d–case study which occurs in the Lotka–Volterra model, see also [11] as
740 a complementary study for the fixed end point problem.

741 *Lie brackets and feedback invariants.* The first step is to compute the collinear set \mathcal{C} defined
 742 by $\det(X(x), Y(x)) = 0$, which takes the form in the original coordinates:

$$743 \quad (4.5) \quad x_1 x_2 (x_1 \kappa_2 - x_2 \kappa_1 + \varepsilon_2 r_1 - \varepsilon_1 r_2) = 0,$$

744 while the singular locus is $\mathcal{S} : x_1 x_2 (\varepsilon_1 x_1 \kappa_2 - \varepsilon_2 x_2 \kappa_1) = 0$ from (4.4) and Lie brackets of length
 745 3 are:

$$\begin{aligned} & [[Y, X], Y](x) = -x_1 (\varepsilon_1^2 x_1 a_{11} - \varepsilon_2^2 x_2 a_{12}) \frac{\partial}{\partial x_1} - x_2 (\varepsilon_1^2 x_1 a_{21} + \varepsilon_2^2 x_2 a_{22}) \frac{\partial}{\partial x_2}, \\ 746 \quad & [[Y, X], X](x) = -x_1 \left(\varepsilon_1 x_1 (r_1 a_{11} + x_2 a_{12} (a_{11} - a_{21})) + \varepsilon_2 x_2 a_{12} (x_1 (a_{21} - a_{11}) + r_2) \right) \frac{\partial}{\partial x_1} \\ & - x_2 \left(\varepsilon_2 x_2 (r_2 a_{22} + x_1 a_{21} (a_{22} - a_{12})) + \varepsilon_1 x_1 a_{21} (x_2 (a_{12} - a_{22}) + r_1) \right) \frac{\partial}{\partial x_2}. \end{aligned}$$

747 The geometric situation that we analyze in our working example is the exceptional case
 748 where we consider the intersection of the collinear locus with the singular locus, which corre-
 749 sponds from (4.5) and (4.4) to intersection of two straight-lines. It corresponds to a generic
 750 interaction between an hyperbolic arc and an elliptic arc.

751 *Constructing a semi-normal form.* The second step is to construct a semi-normal form for
 752 the system. The construction is detailed in [6] but computation are simple in the $2d$ -case.
 753 It consists to choose coordinates such that the intersection is taken as the origin $(0, 0)$, Y is
 754 identified to the constant vector field $Y = \frac{\partial}{\partial x_2}$ (this amounts mainly to choose ln-coordinates)
 755 while the reference singular direction is identified to the straight line $(0x_1)$.

756 Expanding X in the jet space at $(0, 0)$, this leads to analyze the control system:

$$757 \quad (4.6) \quad \dot{x}_1 = -\lambda x_1 + \alpha x_2^2, \quad \dot{x}_2 = u - u_e$$

758 with $u_e \in]-1, 1[$, $|u| \leq 1$, $\lambda > 0$ and $\alpha > 0$.

759 *Properties of the system.* Computing Lie brackets in the new coordinates show relevant
 760 simplification with respect to the previous formulae:

$$\begin{aligned} 761 \quad & X(x) = (-\lambda x_1 + \alpha x_2^2) \frac{\partial}{\partial x_1} - u_e \frac{\partial}{\partial x_2}, \quad Y(x) = \frac{\partial}{\partial x_2}, \\ 762 \quad & [Y, X](x) = -2\alpha x_2 \frac{\partial}{\partial x_1}, \quad [[Y, X], Y](x) = -2\alpha \frac{\partial}{\partial x_1}, \end{aligned}$$

763 and the singular line is given by

$$764 \quad x_2 = 0.$$

765 Restricting to $x_2 = 0$, one has:

$$766 \quad X|_{x_2=0} = -\lambda x_1 \frac{\partial}{\partial x_1}, \quad [[Y, X], Y]|_{x_2=0}(x) = -2\alpha \frac{\partial}{\partial x_1}.$$

767 Hence

$$768 \quad [[Y, X], Y]|_{x_2=0}(x) = \frac{2\alpha}{\lambda x_1} X|_{x_2=0}(x)$$

769 for $x_1 \neq 0$.

770 Therefore, we obtain the following lemmas.

771 **Lemma 4.4.** 1. The origin $(0,0)$ is an abnormal singular arc reduced to a point and
772 the arc $x_1 > 0$ is hyperbolic and the arc $x_1 < 0$ is elliptic.

773 2. The singular control along the line $x_2 = 0$ is given by $u = u_e$ and is constant and
774 strictly admissible since $u_e \in]-1, +1[$.

775 **Lemma 4.5.** The collinear set \mathcal{C} given by $\det(X, Y) = 0$ is the parabola $x_1 = \alpha x_2^2 / \lambda$.

776 **Clock form.** To analyze a $2d$ -time minimal problem with fixed extremities the standard
777 technique is to introduce the clock form $\omega = p dx$ defined outside the collinear set by:

778
$$p \cdot X(x) = 1, \quad p \cdot Y(x) = 0.$$

779 Computing one has $\omega = \frac{1}{-\lambda x_1 + \alpha x_2^2} dx_1$ so that

780
$$d\omega = \frac{2\alpha x_2}{(-\lambda x_1 + \alpha x_2^2)^2} dx_1 \wedge dx_2.$$

781 One can decompose $\mathbb{R}^2 \setminus (\mathcal{C} \cup \mathcal{S})$ in four domains:

- 782 • domain A : $\dot{x}_1 < 0 \cap x_2 > 0$,
783 • domain B : $\dot{x}_1 > 0 \cap x_2 > 0$,
784 • domain C : $\dot{x}_1 < 0 \cap x_2 < 0$,
785 • domain D : $\dot{x}_1 > 0 \cap x_2 < 0$.

786 On each domain one can compare the time along arcs γ_1, γ_2 joining respectively x_0 to x_1
787 where $\gamma_1 = \sigma_+ \sigma_-$, $\gamma_2 = \sigma_- \sigma_+$ using Stokes theorem. One has:

788 **Lemma 4.6.** In domain A and D for such arcs the time minimal policy is $\sigma_- \sigma_+$ while in
789 domain B and C the optimal policy is $\sigma_+ \sigma_-$.

790 **Proof.** Take the case of domain A , one has:

791
$$\int_{\gamma_1} \omega - \int_{\gamma_2} \omega = \int_{\gamma_1 \vee (-\gamma_2)} d\omega > 0,$$

792 hence the time along γ_1 is longer than the time along γ_2 . The discussion is similar for the
793 other cases. ■

794 **Integrating the extremal curves.** The adjoint system takes the form with $p = (p_1, p_2)$:

795
$$\dot{p}_1 = \lambda p_1, \quad \dot{p}_2 = -2\alpha x_2 p_1.$$

796 Denoting for $u = \pm 1$, $\beta = u - u_e$, one gets:

797 **Lemma 4.7.** The extremal system is characterized by:

- 798 • $x_2(t) = x_2(0) + \beta t$,
799 • $x_1(t) = e^{-\lambda t} \left(x_1(0) + \int_0^t e^{\lambda s} (x_2(0) + \beta s)^2 ds \right)$
800 • $p_1(t) = e^{\lambda t} p_1(0)$,
801 • $p_2(t) = -2\alpha p_1(0) \int_0^t e^{\lambda s} (x_2(0) + \beta s) ds$

802 and they belong to the polynomial exponential category.

803 The integrals in the expressions of $x_1(t)$ and $p_2(t)$ can be evaluated using:

$$804 \quad \int_0^t se^{\lambda s} ds = \frac{te^{\lambda t}}{\lambda} - \frac{1}{\lambda^2} (e^{\lambda t} - 1), \quad \int_0^t s^2 e^{\lambda s} ds = \frac{t^2 e^{\lambda t}}{\lambda} - \frac{2}{\lambda} \int_0^t se^{\lambda s} ds.$$

805 **Lemma 4.8.** *The switching function is $\Phi(t) = p_2(t)$ so that for $u = \pm 1$ and one has:*
 806 $\ddot{p}_2(t) = -2\alpha p_1(\lambda x_2 + u - u_e)$ where $p_1(t)$ is of constant sign given by the sign of $p_1(0)$.

807 **Geometric discussion of the synthesis with a terminal manifold N of codimension one.** Next
 808 we present the discussion of the time minimal synthesis with a terminal manifold N of codi-
 809 mension one by gluing cases discussed in [6].

810 One takes N as a circle with radius d centered at 0 where the synthesis amounts to glue
 811 the hyperbolic and elliptic situation. The circle intersects the hyperbolic arc σ_s at $x_1 = d$ and
 812 the elliptic arc σ_s at $x_1 = -d$.

813 The BC-extremals curves can be parameterized by Lemma 4.7 with $(p_1(0), p_2(0)) = \pm n(0)$
 814 where $n(0)$ is the normal to the circle, $n(0) = (x(s), y(s))$. Geodesics curves are integrated
 815 backwards, geodesics in the interior to the circle are associated to $n(0)$ and geodesics exterior
 816 to the circle are associated to $-n(0)$.

817 Since $Y = \frac{\partial}{\partial x_2}$, from [6] we can at once deduced the synthesis outside the circle, near
 818 the hyperbolic point $(d, 0)$ and the elliptic point $(-d, 0)$, using the curvature of N only at
 819 such point which are the images of the curve $(-1/2ks^2, s)$, $k > 0$ at the hyperbolic point and
 $(1/2ks^2, s)$ at the elliptic point. They are represented on Fig. 7.

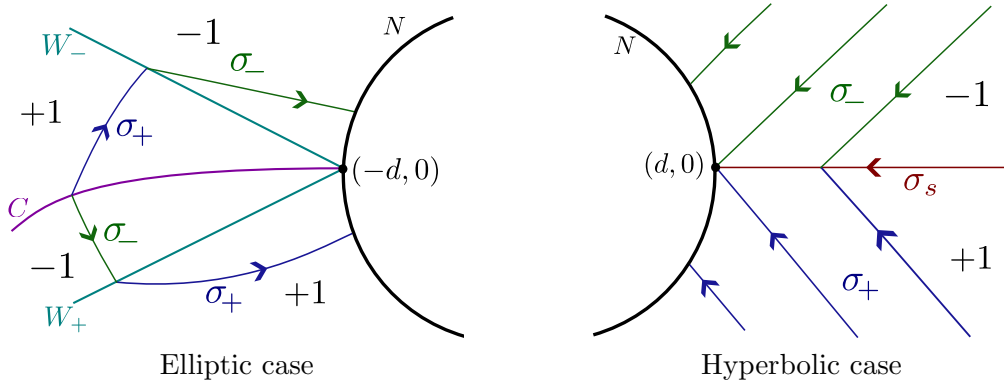


Figure 7. $2d$ -syntheses.

820

821 The main properties are

- 822 • *hyperbolic case:* the singular arc is optimal and the optimal policy is -1 for $x_2 > 0$
 823 and $+1$ for $x_2 < 0$.
- 824 • *elliptic case:* The time minimal synthesis is defined by the stratification $W = W_- \cup W_+$
 825 of the switching locus and there exists a cut locus C terminating at $(-d, 0)$.

826 To complete the analysis one must glue the two syntheses along the target N and consider
 827 also geodesics interior to the circle.

828 Using the analysis of [6] to glue different Whitney charts, we obtain the time minimal
 829 synthesis in a neighborhood V of the origin, which is schematically represented in Fig. 8.

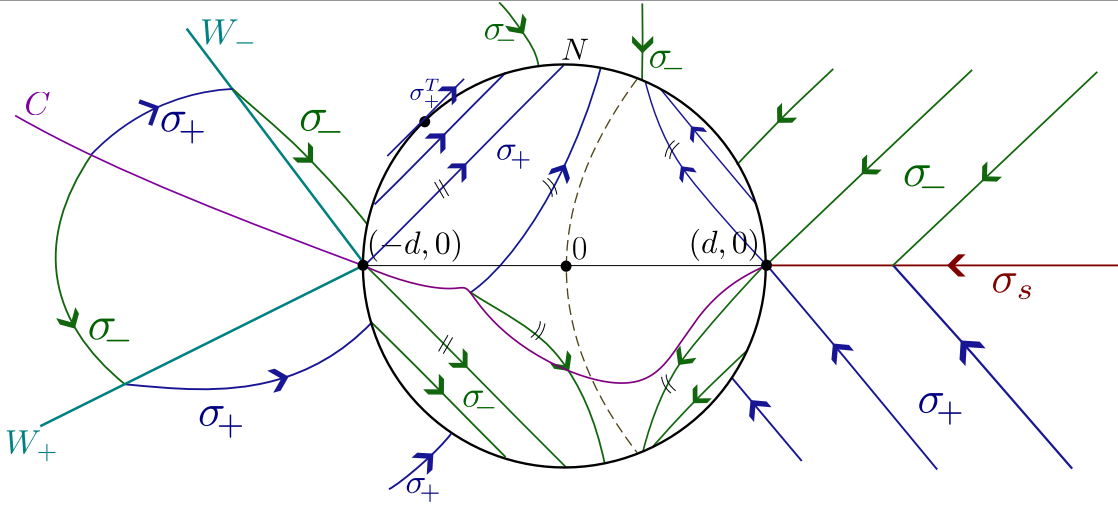


Figure 8. Schematic representation of the time minimal synthesis gluing hyperbolic and elliptic case with N being the unit circle. The cut locus was numerically computed with parameters $\lambda = \alpha = 1$ and $u_e = 1/2$.

830 **4.4.2. Complexity of the singular flow in the 3d-case.** From dynamical system point
831 of view, the complexity of the Lotka–Volterra model is related to the existence of persistent
832 equilibrium point, which leads to complicated dynamics related to the hierarchy of dynamics
833 associated to the hierarchy of at most 2^n –equilibria.

834 Hence, in this section one analyses the same question regarding to existence of permanent
835 equilibria for the singular dynamics associated to the time minimal control problem.

836 First one must extent the previous $2d$ –result concerning the existence of (exceptional)
837 singular arc reduced to a point, in the context of controlled Lotka–Volterra model.

838 **Proposition 4.9.** Consider the controlled Lotka–Volterra model in the n –dimensional case.
839 Then there exists (isolated) exceptional arcs reduced to a point.

840 *Proof.* Consider the pair (X, Y) , and choose ln–coordinates so that $Y(x) = \frac{\partial}{\partial x_n}$ with
841 $X(x) = \sum_{i=1}^n X_i(x) \frac{\partial}{\partial x_i}$, the collinear set is defined by the $(n - 1)$ –equations $X_i(x) = 0$,
842 $i = 1, \dots, n - 1$ and let $\lambda = -u_e$ so that $X_n(x) = -\lambda$. Let $\tilde{X}(x) = \sum_{i=1}^{n-1} X_i(x) \frac{\partial}{\partial x_i} +$
843 $(X_n(x) + u_e) \frac{\partial}{\partial x_n}$ and by construction there exists x_e on the collinear set so that $\tilde{X}(x_e) = 0$.
844 Denote by \tilde{J} the *Jacobian matrix* of \tilde{X} at $x = x_e$ and let $\sigma(\tilde{J})$ be its spectrum.

845 Denoting by $\text{ad} \tilde{X} \cdot Y = [\tilde{X}, Y]$. Then at x_e the matrix with columns of iterated Lie brackets

846
$$K = \left(Y, \text{ad} \tilde{X} \cdot Y, \dots, \text{ad}^{n-1} \tilde{X} \cdot Y \right)$$

847 coincides with the *Kalman matrix*

848
$$\left(b, \tilde{J}b, \dots, \tilde{J}^{n-1}b \right)$$

849 where b is the constant vector $Y(x)$. The singular point is exceptional if and only if $\text{rank} K \leq$
850 $n - 1$.

851 At isolated point, the condition $\text{rank} = n - 1$ can be realized for the controlled Lotka–
852 Volterra model (see Example 4.10 for $n = 3$). ■

853 *Example 4.10.* In the dimensionless coordinates (see Proposition 4.1), take: $A = \text{diag}(\lambda_1,$
854 $\lambda_1, \lambda_3)$, $X(x) = -\text{diag}(x + 1) Ax$, $Y(x) = \text{diag}(x + 1) (\varepsilon_1, \varepsilon_2, \varepsilon_3)^\top$ so that the persistent equi-
855 librium is located at $x_e = 0$. The columns of the Kalman matrix K defined in the proof of
856 Proposition 4.9 are

$$\begin{aligned} 857 \quad Y(0) &= (\varepsilon_1, \varepsilon_2, \varepsilon_3)^\top, \\ 858 \quad [X, Y](0) &= (-\varepsilon_1 \lambda_1, -\varepsilon_2 \lambda_1, -\varepsilon_3 \lambda_3)^\top, \\ 859 \quad [X, [X, Y]](0) &= (\varepsilon_1 \lambda_1^2, +\varepsilon_2 \lambda_1^2, \varepsilon_3 \lambda_3^2)^\top, \end{aligned}$$

860 hence $\text{rank} K < 3$ and 0 is a singular exceptional point.

861 Note that the Jacobian matrix of the singular flow, defined for $\varepsilon_1 \neq \varepsilon_2$, evaluated at 0 is

$$862 \quad J = \begin{pmatrix} \frac{\varepsilon_1 \lambda_3}{\varepsilon_1 - \varepsilon_2} - \lambda_1 & \frac{\varepsilon_1 \lambda_3}{\varepsilon_2 - \varepsilon_1} & 0 \\ \frac{\varepsilon_2 \lambda_3}{\varepsilon_1 - \varepsilon_2} & \frac{\varepsilon_1 \lambda_3}{\varepsilon_2 - \varepsilon_1} - \lambda_1 + \lambda_3 & 0 \\ \frac{\varepsilon_3 \lambda_3}{\varepsilon_1 - \varepsilon_2} & -\frac{\varepsilon_3 \lambda_3}{\varepsilon_1 - \varepsilon_2} & -\lambda_3 \end{pmatrix}$$

863 and its spectrum $\{\lambda_3 - \lambda_1, -\lambda_3, -\lambda_1\}$ is resonant.

864 *3d-case.* In the 3d-case, the singular trajectories are solutions of the vector field: $\dot{x} =$
865 $X_s(x) = X(x) - u_s Y(x)$, where the singular control feedback is $u_s = -D'(x)/D(x)$ with

$$866 \quad D(x) = \det(Y(x), [Y, X](x), [[Y, X], Y](x)), \quad D'(x) = \det(Y(x), [Y, X](x), [[Y, X], X](x)).$$

867 Moreover exceptional trajectories are located on the exceptional locus $D''(x) = 0$ with

$$868 \quad D''(x) = \det(Y(x), [Y, X](x), X(x)).$$

869 Computing in the original coordinates leads to complicated expressions:

$$\begin{aligned} 870 \quad D(x)/x_1 x_2 x_3 &= (\varepsilon_1^2 x_1 a_{21} + \varepsilon_1 (\varepsilon_2 (x_2 a_{22} - x_1 a_{11}) + \varepsilon_3 x_3 a_{23}) - \varepsilon_2 (\varepsilon_2 x_2 a_{12} + \varepsilon_3 x_3 a_{13})) \\ 871 \quad &(\varepsilon_1^2 x_1 a_{31} + \varepsilon_2^2 x_2 a_{32} + \varepsilon_3^2 x_3 a_{33}) + (\varepsilon_1^2 x_1 a_{11} + \varepsilon_2^2 x_2 a_{12} + \varepsilon_3^2 x_3 a_{13}) (\varepsilon_2^2 x_2 a_{32} + \varepsilon_3 \varepsilon_2 (x_3 a_{33} - x_2 a_{22}) \\ 872 \quad &- \varepsilon_3^2 x_3 a_{23} + \varepsilon_1 x_1 (\varepsilon_2 a_{31} - \varepsilon_3 a_{21})) - (\varepsilon_1^2 x_1 a_{21} + \varepsilon_2^2 x_2 a_{22} + \varepsilon_3^2 x_3 a_{23}) \\ 873 \quad &(\varepsilon_1^2 x_1 a_{31} + \varepsilon_1 (\varepsilon_2 x_2 a_{32} + \varepsilon_3 (x_3 a_{33} - x_1 a_{11})) - \varepsilon_3 (\varepsilon_2 x_2 a_{12} + \varepsilon_3 x_3 a_{13})), \end{aligned}$$

874

$$\begin{aligned} 875 \quad D'(x)/x_1 x_2 x_3 &= (-\varepsilon_1^2 x_1 a_{21} + \varepsilon_1 (\varepsilon_2 (x_1 a_{11} - x_2 a_{22}) - \varepsilon_3 x_3 a_{23}) + \varepsilon_2 (\varepsilon_2 x_2 a_{12} + \varepsilon_3 x_3 a_{13})) \\ 876 \quad &(\varepsilon_2 x_2 (x_1 a_{12} a_{31} - a_{32} (x_1 a_{21} + x_3 (a_{23} - a_{33}) + r_2)) - \varepsilon_1 x_1 (r_1 a_{31} + x_3 (a_{13} - a_{33}) a_{31} \\ 877 \quad &+ x_2 (a_{12} a_{31} - a_{21} a_{32})) + \varepsilon_3 x_3 (-r_3 a_{33} + x_1 a_{31} (a_{13} - a_{33}) + x_2 a_{32} (a_{23} - a_{33}))) \\ 878 \quad &+ (\varepsilon_2^2 (-x_2) a_{32} + \varepsilon_3 \varepsilon_2 (x_2 a_{22} - x_3 a_{33}) + \varepsilon_3^2 x_3 a_{23} + \varepsilon_1 x_1 (\varepsilon_3 a_{21} - \varepsilon_2 a_{31})) \\ 879 \quad &(-\varepsilon_1 x_1 (r_1 a_{11} + x_2 a_{12} (a_{11} - a_{21}) + x_3 a_{13} (a_{11} - a_{31})) + \varepsilon_2 x_2 (x_3 a_{13} a_{32} - a_{12} (x_1 (a_{21} - a_{11}) \\ 880 \quad &+ x_3 a_{23} + r_2)) - \varepsilon_3 x_3 (a_{13} (x_1 (a_{31} - a_{11}) + x_2 a_{32} + r_3) - x_2 a_{12} a_{23})) \end{aligned}$$

$$\begin{aligned}
 & - (\varepsilon_1^2 (-x_1) a_{31} + \varepsilon_1 (\varepsilon_3 (x_1 a_{11} - x_3 a_{33}) - \varepsilon_2 x_2 a_{32}) + \varepsilon_3 (\varepsilon_2 x_2 a_{12} + \varepsilon_3 x_3 a_{13})) \\
 & (\varepsilon_1 x_1 (x_3 a_{23} a_{31} - a_{21} (x_3 a_{13} + x_2 (a_{12} - a_{22}) + r_1)) + \varepsilon_2 x_2 (-r_2 a_{22} + x_1 a_{21} (a_{12} - a_{22}) \\
 & + x_3 a_{23} (a_{32} - a_{22})) + \varepsilon_3 x_3 (x_1 a_{13} a_{21} - a_{23} (x_1 a_{31} + x_2 (a_{32} - a_{22}) + r_3))),
 \end{aligned}$$

$$\begin{aligned}
 D''(x)/x_1 x_2 x_3 = & (-\varepsilon_1^2 x_1 a_{21} + \varepsilon_1 (\varepsilon_2 (x_1 a_{11} - x_2 a_{22}) - \varepsilon_3 x_3 a_{23}) + \varepsilon_2 (\varepsilon_2 x_2 a_{12} + \varepsilon_3 x_3 a_{13})) \\
 & (x_1 a_{31} + x_2 a_{32} + x_3 a_{33} + r_3) + (-\varepsilon_2^2 x_2 a_{32} + \varepsilon_3 \varepsilon_2 (x_2 a_{22} - x_3 a_{33}) + \varepsilon_3^2 x_3 a_{23} + \varepsilon_1 x_1 (\varepsilon_3 a_{21} \\
 & - \varepsilon_2 a_{31})) (x_1 a_{11} + x_2 a_{12} + x_3 a_{13} + r_1) + (\varepsilon_1^2 x_1 a_{31} + \varepsilon_1 (\varepsilon_2 x_2 a_{32} + \varepsilon_3 (x_3 a_{33} - x_1 a_{11})) \\
 & - \varepsilon_3 (\varepsilon_2 x_2 a_{12} + \varepsilon_3 x_3 a_{13})) (x_1 a_{21} + x_2 a_{22} + x_3 a_{23} + r_2).
 \end{aligned}$$

Proposition 4.11. *If $D(x) \neq 0$, the equilibria of the singular dynamics $\dot{x} = X_s(x)$ are exceptional trajectories reduced to a point. At such a point x_e , the spectrum of $J = \frac{\partial X_s}{\partial x}(x_e)$ is a feedback invariant. Moreover the dynamics is foliated by the invariant set $D''(x) = 0$ and $D(x)D''(x) > 0$ or < 0 associated respectively to hyperbolic and elliptic arcs. The singular feedback u_s acts as a geometric pole placement of the dynamics on the collinear set.*

Proof. The proof is clear following the construction detailed in the proof of Proposition 4.9. ■

4.4.3. The 4d-case. This gives the road to the n -dimensional case.

The singular exceptional control can be expressed as a feedback using the relation

$$\begin{aligned}
 H_X(z) = H_Y(z) = \{H_X, H_Y\}(z) = 0 \\
 \{\{H_X, H_Y\}, H_X\}(z) + u_{se} \{\{H_X, H_Y\}, H_Y\}(z) = 0
 \end{aligned}$$

and this leads to

$$u_{se}(x) = -\frac{D'(x)}{D(x)},$$

where

$$\begin{aligned}
 D(x) &= \det(X(x), Y(x), [Y, X](x), [[Y, X], Y](x)), \\
 D'(x) &= \det(X(x), Y(x), [Y, X](x), [[Y, X], X](x)).
 \end{aligned}$$

Similarly to the 3d-case, the singular exceptional dynamics: $\dot{x} = X(x) + u_{se}Y(x)$ can be used to generate feedback invariants.

Remaining singular dynamics are parameterized by a dynamic feedback $u(x, \lambda)$ depending upon a one dimensional coefficient.

We refer to [9] for a general approach to compute feedback invariants for the dynamics.

5. Conclusion. In this article we have presented the general techniques from geometric control to analyze in the permanent case, the optimal control problem related to vermin reduction in a complex microbiote modelled by the Lotka–Volterra equations.

Our analysis is based on a series of articles classifying the time minimal syntheses for a single-input affine system with terminal manifold of codimension one developed for chemical networks [6, 7, 21]. Using the concepts of Whitney chart and unfolding the explicit computations in a neighbourhood of the terminal manifold can be reduced to problems in dimension 2

Barnesiella (Bar.)						0.3680	Akkermansia (Akk.)					0.2297
undefined genus of Lachnospiraceae (Und. Lac.)						0.3102	Coprobacillus (Cop.)					0.8300
undefined genus of unclassified Mollicutes (Und. Mol.)						0.4706	Clostridium difficile (C. diff.)					0.3918
unclassified Lachnospiraceae (Uncl. La.)						0.3561	Enterococcus (Ent.)					0.2907
Blautia (Bla.)						0.7089	undefined genus of Enterobacteriaceae (Und. En.)					0.3236
Other						0.5400						
	Bar.	Und. Lac.	Uncl. Lac.	Other	Bla.	Und. Mol.	Akk.	Cop.	Und. En.	Ent.	C. diff.	
Bar.	-0.205	0.098	0.167	-0.164	-0.143	0.019	-0.515	-0.391	-0.268	0.008	0.346	
Und. Lac.	0.062	-0.104	-0.043	-0.154	-0.187	0.027	-0.459	-0.413	-0.196	0.022	0.301	
Uncl. Lac.	0.143	-0.192	-0.101	-0.139	-0.165	0.013	-0.504	-0.772	-0.206	-0.006	0.292	
Other	0.224	0.138	0.000	-0.831	-0.223	0.220	-0.205	-1.009	-0.400	-0.039	0.666	
Bla.	-0.180	-0.051	0.000	-0.054	-0.708	0.016	-0.507	0.553	0.106	0.224	0.157	
Und. Mol.	-0.111	-0.037	-0.042	0.041	0.261	-0.422	-0.185	-0.432	-0.264	-0.061	0.164	
Akk.	-0.126	-0.185	-0.122	0.380	0.400	-0.160	-1.212	1.389	-0.096	0.191	-0.379	
Cop.	-0.071	0.000	0.080	-0.454	-0.503	0.169	-0.562	-4.350	-0.207	-0.223	0.443	
Und. Ent.	-0.374	0.278	0.248	-0.168	0.084	0.033	-0.232	-0.395	-0.384	-0.038	0.314	
Ent.	-0.042	-0.013	0.024	-0.117	-0.328	0.020	0.054	-2.096	0.023	-0.192	0.111	
C. diff.	-0.037	-0.033	-0.049	-0.090	-0.102	0.032	-0.181	-0.303	-0.007	0.014	-0.055	

Table 1

(top) Growth rates a_{ij} of each microbial population i of the CDI model. (bottom) Interactions between pairwise microbial populations of the CDI model. Both tables are excerpted from [27].

917 or 3 and a dictionary of the time minimal syntheses is described in [6, 21], up to codimension
 918 2 cases. Global syntheses can be described by gluing different Whitney charts.

919 It can be applied to the controlled Lotka–Volterra model to analyze either the problem
 920 of reducing the infection using an antibiotic agent or to reinforce the body prior to infection
 921 using a probiotic agent. A case study is given to construct a global optimal synthesis by gluing
 922 distinct Whitney charts.

923 Our article shows the parallel between the analysis of the free dynamics in the frame of dy-
 924 namical systems and the dynamics of the Hamiltonian dynamics deduced from the Maximum
 925 Principle which parameterizes the extremals candidates as minimizers.

926 The complexity of the Hamiltonian dynamics for nonlinear control systems is related to
 927 the existence and their complexity of the singular extremals dynamics. Our contribution is to
 928 present preliminary analysis of this complexity, in the frame of the controlled Lotka–Volterra
 929 model. It is shown to be related to the collinear set on which are located the equilibrium of
 930 the free dynamics, where no treatment is applied, and the forced equilibrium associated to
 931 maximal treatment.

932 An additional step in our analysis will be to analyze the problem in the sampled–data
 933 control frame in relation with the permanent case, see [8] for such an analysis.

934

REFERENCES

- 935 [1] A.A. AGRACHEV, Y.L. SACHKOV, *Control theory from the geometric viewpoint*. Encyclopaedia of
 936 Mathematical Sciences, 87. Control Theory and Optimization, II. Springer-Verlag, Berlin, 2004, 412
 937 pages.
 938 [2] F. ANCONA, A. BRESSAN, *Nearly time optimal stabilizing patchy feedbacks*. Ann. Inst. H. Poincaré Anal.
 939 Non Linéaire **24** no. 2 (2007), pp. 279–310.

- 940 [3] S. BAIGENT, *Geometry of carrying simplices of 3-species competitive Lotka–Volterra systems*. Nonlinearity,
941 **26** no. 4 (2013), pp. 1001–1029.
- 942 [4] B. BONNARD, M. CHYBA, *The role of singular trajectories in control theory*. Springer Verlag, New York,
943 2003, 357 pages.
- 944 [5] B. BONNARD, I. KUPKA, *Théorie des singularités de l’application entrée/sortie et optimalité des trajec-*
945 *toires singulières dans le problème du temps minimal*. Forum Math. **5** no. 2 (1993), pp. 111–159.
- 946 [6] B. BONNARD, G. LAUNAY, M. PELLETIER, *Classification générique de synthèses temps minimales avec*
947 *cible de codimension un et applications*. Annales de l’I.H.P. Analyse non linéaire **14** no.1 (1997), pp.
948 55–102.
- 949 [7] B. BONNARD, J. ROUOT, *Towards Geometric Time Minimal Control without Legendre Condition and*
950 *with Multiple Singular Extremals for Chemical Networks*. Advances in Nonlinear Biological Systems,
951 Modeling and Optimal Control, AIMS on applied Maths **11** (2021), pp. 1–34.
- 952 [8] B. BONNARD, J. ROUOT, C. SILVA, *Geometric Optimal Control of the Generalized Lotka–Volterra Model*
953 *of the Intestinal Microbiome*. Preprint 2023: [hal-03861565](https://hal.archives-ouvertes.fr/hal-03861565).
- 954 [9] B. BONNARD, J. ROUOT, *Feedback Classification and Optimal Control with Applications to the Controlled*
955 *Lotka–Volterra Model*. Preprint 2023: [hal-03917363](https://hal.archives-ouvertes.fr/hal-03917363).
- 956 [10] V.G. BOLTYANSKII, *Sufficient conditions for optimality and the justification of the dynamic programming*
957 *method*. SIAM J. Control **4** (1966), pp. 326–361.
- 958 [11] U. BOSCAIN, B. PICCOLI, *Optimal syntheses for control systems on 2-D manifolds*. Springer Science &
959 Business Media **43** 2003, 275 pages.
- 960 [12] P. BRUNOVSKÝ, *Existence of regular synthesis for general control problems*. J. Differential Equations **38**
961 no. 3 (1980), pp. 317–343.
- 962 [13] W.L. CHOW, *Über Systeme von linearen partiellen Differentialgleichungen erster Ordnung*. Mathematis-
963 che Annalen, **117** (1939) pp. 98–105.
- 964 [14] I. EKELAND, *Discontinuités de champs hamiltoniens et existence de solutions optimales en calcul des*
965 *variations*. Inst. Hautes Études Sci. Publ. Math. **47** (1977), pp. 5–32.
- 966 [15] M. FEINBERG, *Foundations of chemical reaction network theory*. Applied Mathematical Sciences, 202.
967 Springer, Cham, 2019, 454 pages.
- 968 [16] M.W. HIRSCH, *Systems of differential equations which are competitive or cooperative: III. Competing*
969 *species*. Nonlinearity, **1**, (1988), pp.51–71.
- 970 [17] E.W. JONES, P. S. CLARCKE, J. M. CARSLON, *Navigation of outcome in a generalized Lotka–Volterra*
971 *model of the microbiome*. Advances in Nonlinear Biological Systems, Modeling and Optimal Control,
972 AIMS on applied Maths **11** (2021), pp. 97–117.
- 973 [18] A.J. KRENER, *The high order maximal principle and its application to singular extremals*. SIAM J.
974 Control Optim. **15** no.2 (1977), pp. 256–293.
- 975 [19] I. KUPKA, *Geometric theory of extremals in optimal control problems. I. The fold and Maxwell case*.
976 Trans. Amer. Math. Soc. **299** no.1 (1987), pp. 225–243.
- 977 [20] I. KUPKA, *The ubiquity of Fuller’s phenomenon*. Nonlinear controllability and optimal control, 313–350,
978 Monogr. Textbooks Pure Appl. Math., 133, Dekker, New York, 1990.
- 979 [21] G. LAUNAY, M. PELLETIER, *The generic local structure of time-optimal synthesis with a target of*
980 *codimension one in dimension greater than two*. Journal of Dynamical and Control Systems **3**, no.
981 165 (1997).
- 982 [22] E.B. LEE, L. MARKUS, *Foundations of optimal control theory*. John Wiley & Sons, Inc., New York-
983 London-Sydney 1967, 576 pages.
- 984 [23] A.J. LOTKA, *Elements of mathematical biology*. Dover Publications, Inc., New York, N.Y., 1958, 465
985 pages.
- 986 [24] L.S. PONTRYAGIN, V.G. BOLTYANSKII, R.V. GAMKRELIDZE, E.F. MISHCHENKO, *The mathematical*
987 *theory of optimal processes*. Oxford, Pergamon Press, 1964, 362 pages.
- 988 [25] H. SCHÄTTLER, U. LEDZEWICZ, *Optimal control for mathematical models of cancer therapies. An appli-*
989 *cation of geometric methods*. Interdisciplinary Applied Mathematics, 42. Springer, New York, 2015,
990 496 pages.
- 991 [26] S. SMALE, *On the differential equations of species in competition*. Journal of Mathematical Biology, **3**
992 (1976), pp. 5–7.
- 993 [27] R.R. STEIN, V. BUCCI, N.C. TOUSSAINT, C.G. BUFFIE, G. RÄTSCH, E.G. PAMER, ET AL., *Ecological*

- 994 *modelling from time-series inference: insight into dynamics and stability of intestinal microbiota.*
995 PLoS Comp. Biology, **9** no. 12 (2013).
- 996 [28] V. VOLTERRA, *Leçons sur la théorie mathématique de la lutte pour la vie.* Les Grands Classiques
997 Gauthier-Villars. Éditions Jacques Gabay, Sceaux, 1990, 215 pages.
- 998 [29] E.C. ZEEMAN, M.L. ZEEMAN, *From local to global behavior in competitive Lotka Volterra systems.* Trans.
999 Amer. Math. Soc., 355 (2003), pp. 713–734.